Final Report

BOUNDARY CONDITIONS AND FIRE EMISSIONS MODELING

Work Order No. 582-07-84005-FY08-10

Prepared for

Texas Commission on Environmental Quality
12118 Park 35 Circle
Austin, Texas 78753

Prepared by

Edward Tai
Michele Jimenez
Ou Nopmongcol
Gary Wilson
Gerry Mansell
Bonyoung Koo
Greg Yarwood

ENVIRON International Corporation
773 San Marin Drive, Suite 2115
Novato, CA 94998

September 2008

TABLE OF CONTENTS

Page

EXECUTIVE SUMMARY ES-1

1. INTRODUCTION 1-1

2. DEVELOPMENT OF FIRE EMISSIONS 2-1

2.1. NCAR Episodic Fire Emissions 2-1
2.2. Typical Fires 2-6
2.3. Processing Fire Emissions Using EPS3 2-9

3. CAMx MODELING 3-1

3.1. CAMx Inputs 3-2
3.3. CAMx Results 3-7

4. CAMx FUTURE YEAR MODELING 4-1

4.1. Typical Fire Emissions 4-1
4.2. Future Year Results 4-4

REFERENCES R-1

TABLES

Table 2-1. Fire classes used by WRAP 2-2
Table 2-2. Comparison of virtual area and PM2.5 emission bins 2-3
Table 2-3. Number of fire points and total PM2.5 emissions for June and July 2-5
Table 2-4. EPS3 input format for point source fire emissions 2-6
Table 2-5. List of the typical fire files in SMOKE-format for area sources (top) and point sources (bottom) for each region 2-7
Table 2-6. Factors used to convert TOG to CB05 species for fire emissions 2-10
Table 2-7. Fire-related parameters as a function of fire size class 2-15
Table 2-8. Buoyancy efficiency as a function of hour of day 2-16
Table 2-9. Vertical layer structure for the 19-layer RPO domain 2-17
Table 2-10. Landuse/Landcover descriptions 2-22
Table 2-11. Cropland data sources by state used for surrogate development in the TCEQ domain. 2-24
Table 2-12. Spatial surrogate definitions 2-25
Table 2-13. Surrogate/SCC assignments for spatial allocation of fire emissions 2-28

Table 3-1. List of MOZART species available in 2005 3-3
Table 3-2. Mapping of MOZART to CAMx CB05 species 3-4
Table 3-3. Mapping of GEOS-Chem to CAMx CB05 species 3-5
Table 3-4. Top boundary conditions (ppm for gases, ug/m^3 for aerosols) 3-6

Table 3-5. Height interfaces of the RPO and TCEQ vertical layer structures 3-7

Table 4-1. Typical area source fire emissions for a weekday from May to October..... 4-2
Table 4-2. Typical point source fire emissions on five Wednesdays..... 4-3
Table 4-3. Typical vs. satellite-derived fire emissions..... 4-4
Table 4-4. Fire and total NOx emissions in the base and future years..... 4-4

FIGURES

Figure ES-1. Map of the national RPO 36 km domain, the TCEQ's eastern US 36 km domain, and ozone monitoring locations near the TCEQ domain boundaries.....ES-1
Figure ES-2. Time series of differences in daily ozone at monitoring sites near the boundaries of the TCEQ 36 km domain between 2005 and 2018 (top) and 2006 and 2018 (bottom) ES-3

Figure 2-1. Fire point distribution before and after grouping points within 5 km of one another 2-2
Figure 2-2. Fire point distribution when the maximum grouping distance is 5 km and 3 km..... 2-3
Figure 2-3. Comparison of fire classes sorted by virtual acreage, virtual acreage cut by 50% for individual fire points, and daily PM2.5 emissions..... 2-4
Figure 2-4. Scatterplot of fire points comparing daily PM2.5 emissions to the virtual area 2-4
Figure 2-5. Diurnal profiles of Fire Class 4 plume top and plume bottom in the CENRAP, WRAP, and VISTAS typical fire inventory..... 2-8
Figure 2-6. PM2.5 speciation profiles 2-10
Figure 2-7. Standard diurnal distribution of daily fire emissions..... 2-11
Figure 2-8. Monthly profiles of agricultural burning of corn in northern and southern CENRAP states 2-12
Figure 2-9. Monthly profiles of agricultural burning in VISTAS states 2-13
Figure 2-10. Allocation of agricultural burning emissions by day of week in the CENRAP states for all crops..... 2-13
Figure 2-11. Diurnal agricultural burning profiles 2-14
Figure 2-12. Diurnal profiles of wildfires and prescribed fires in Texas and in the US 2-15
Figure 2-13. Fraction of emissions assigned to the surface emissions file by fire class..... 2-16
Figure 2-14. Vertical layer allocation of fire point sources by hour of the day for each fire class..... 2-18
Figure 2-15. 2007 Cropland Data Layer for the Midwest and Lower Mississippi Valley..... 2-21
Figure 2-16. 36-km gridding surrogates for TCEQ Fire sources. Surrogate 19 – ALL – All Crops..... 2-26
Figure 2-17. 12-km gridding surrogates for TCEQ Fire sources. Surrogate 19 – ALL – All Crops..... 2-27

Figure 3-1. Map of the 36 km RPO and TCEQ domains 3-1
Figure 3-2. Map of AQS ozone monitoring sites near the TCEQ 36 km boundary 3-9
Figure 3-3. Normalized bias and error for 1-hour ozone at monitors near TCEQ's western, southern, and northern boundaries during the May 19-June 3, 2005 episode 3-10
Figure 3-4. Normalized bias and error for 1-hour ozone at monitors near TCEQ's western, southern, and northern boundaries during the June 17 - 30, 2005 episode. 3-11
Figure 3-5. Normalized bias and error for 1-hour ozone at monitors near TCEQ's western, southern, and northern boundaries during the July 26 – August 8, 2005 episode 3-12
Figure 3-6. Normalized bias and error for 1-hour ozone at monitors near TCEQ's western, southern, and northern boundaries during the May 31 to June 16, 2006 episode 3-14
Figure 3-7. Normalized bias and error for 1-hour ozone at monitors near TCEQ's western, southern, and northern boundaries during the August 1 – October 15, 2006 episode 3-19
Figure 3-8. Ozone contributions from top and lateral boundaries from an inert run during the May 19 to June 3, 2005 episode 3-21
Figure 3-9. Ozone contributions from top and lateral boundaries from an inert run during the June 17-30, 2005 episode 3-21
Figure 3-10. Ozone contributions from top and lateral boundaries from an inert run in the July 26 – August 8, 2005 episode 3-22
Figure 3-11. Ozone contributions from top and lateral boundaries from an inert run in the May 31 – June 16, 2006 episode 3-22
Figure 3-12. Ozone contributions from top and lateral boundaries from an inert run in the August 1 – October 15, 2006 episode 3-23

Figure 4-1. Time series of multi-site and daily averaged ozone in 2005 and 2018 near the western (top), southern (middle), and northern (bottom) boundaries of the TCEQ domain 4-5
Figure 4-2. Time series of the differences in daily average O3 between 2005 and 2018 at sites near the TCEQ 36 km boundaries 4-6
Figure 4-3. Time series of multi-site and daily averaged ozone in 2006 and 2018 near the western (top), southern (middle), and northern (bottom) boundaries of the TCEQ domain 4-7
Figure 4-4. Time series of the differences in daily average O3 between 2006 and 2018 at sites near the TCEQ 36 km boundaries. 4-8

EXECUTIVE SUMMARY

Biomass burning can emit substantial amounts of particulate matter, NOx, and VOCs, which have the potential to significantly increase ozone production downwind of each fire.
To address fire emissions that could be transported into the TCEQ domain, fire emissions must be represented in the lateral boundary conditions. TCEQ domain boundary conditions were developed by performing CAMx simulations on a continental-scale 36 km domain (Figure ES-1) developed by several Regional Planning Organizations (RPOs). Boundary conditions for the continental scale RPO grid were, in turn, extracted from two global models. Modeling was performed for base years (2005 and 2006) and for a future year (2018).

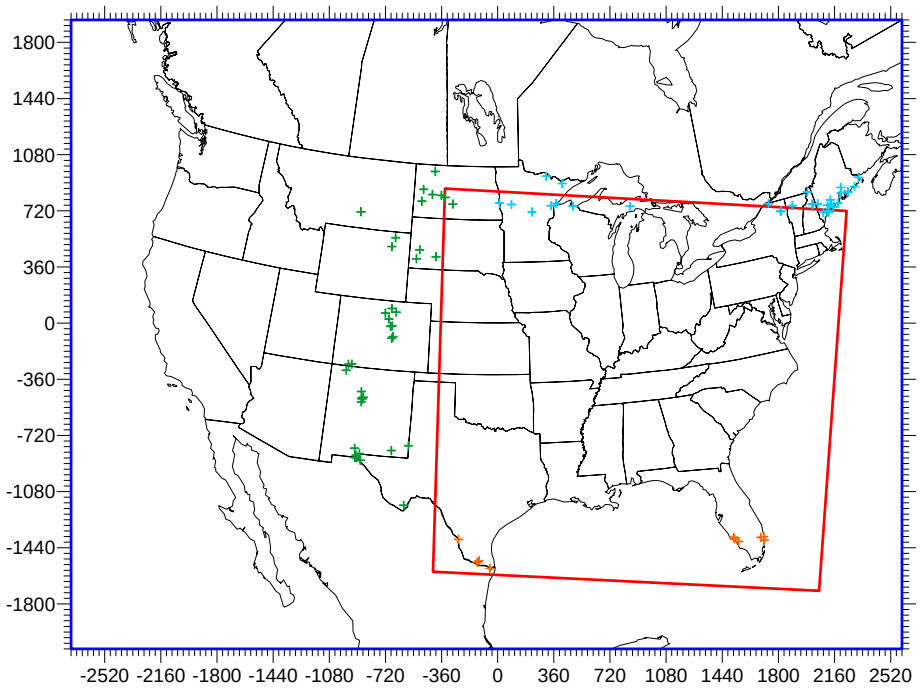

Figure ES-1. Map of the national RPO 36 km domain, the TCEQ's eastern US 36 km domain, and ozone monitoring locations near the TCEQ domain boundaries.

New modules called PREFIR and PSTFIR were developed for the Emissions Processing System (EPS3) specifically to handle point source fire emissions. EPS3 allows each fire point source to be distributed into multiple vertical layers to better represent each fire plume. Day-specific fire emissions for 2005 and 2006 were developed from the National Center for Atmospheric Research (NCAR) satellite-derived fire emissions inventory which was processed for the RPO 36 km domain using EPS3. Typical (i.e., representing a typical year) fire emissions were developed from the Central Regional Air Planning Association (CENRAP) Typical 02g inventory which was also processed in EPS3 for the RPO domain.

The CAMx 2005 and 2006 base year runs in the RPO domain used day-specific NCAR fire data and continental boundary conditions derived from both the GEOS-Chem and MOZART global models. The use of MOZART boundary conditions led to higher surface ozone at monitoring sites near the TCEQ 36 km boundaries and produced slightly better agreement with observed ozone than using GEOS-Chem boundary conditions, especially at sites near TCEQ's western boundary.

The CAMx 2018 future year runs in the RPO domain incorporated the CENRAP typical fire emissions and MOZART boundary conditions. Changes between base and future year ozone near the TCEQ domain boundaries (Figure ES-2) are attributable to changes in anthropogenic emissions and differences between the day-specific (base year) and typical (future year) fire emissions. Future year ozone near TCEQ's western boundary decreased up to 2 ppb compared to the base year on most dates. Future year ozone near TCEQ's southern boundary fluctuated between ±4 ppb from the base year values. Near the northern boundary, future year ozone was lower on most dates, decreasing by as much as 12 ppb, most likely because of declines in ozone outflow across the northern boundary due to anthropogenic emission decreases.

Recommendations

The future year boundary conditions for the TCEQ domain developed in this study could be improved by accounting for changes in background ozone at the scale of continental North America. The MOZART and GEOS-Chem global models were used to specify the boundary conditions for simulations on the national RPO grid and the same global simulations were used for the base and future years. Results from future year MOZART and/or GEOS-Chem modeling could be used to incorporate anticipated changes in continental background ozone resulting, for example, from emission changes in Asia.

The new EPS3 modules for point source fires (PREFIR and PSTFIR) account for plume rise to correctly represent the impacts of fires on both local and transported ozone. In contrast, fires that are inventoried as area sources (e.g., agricultural burning) are modeled as surface sources even though they will have plume rise. Modeling the air quality impacts of area source fires would be improved by developing methods and tools to include plume rise for area source fires.

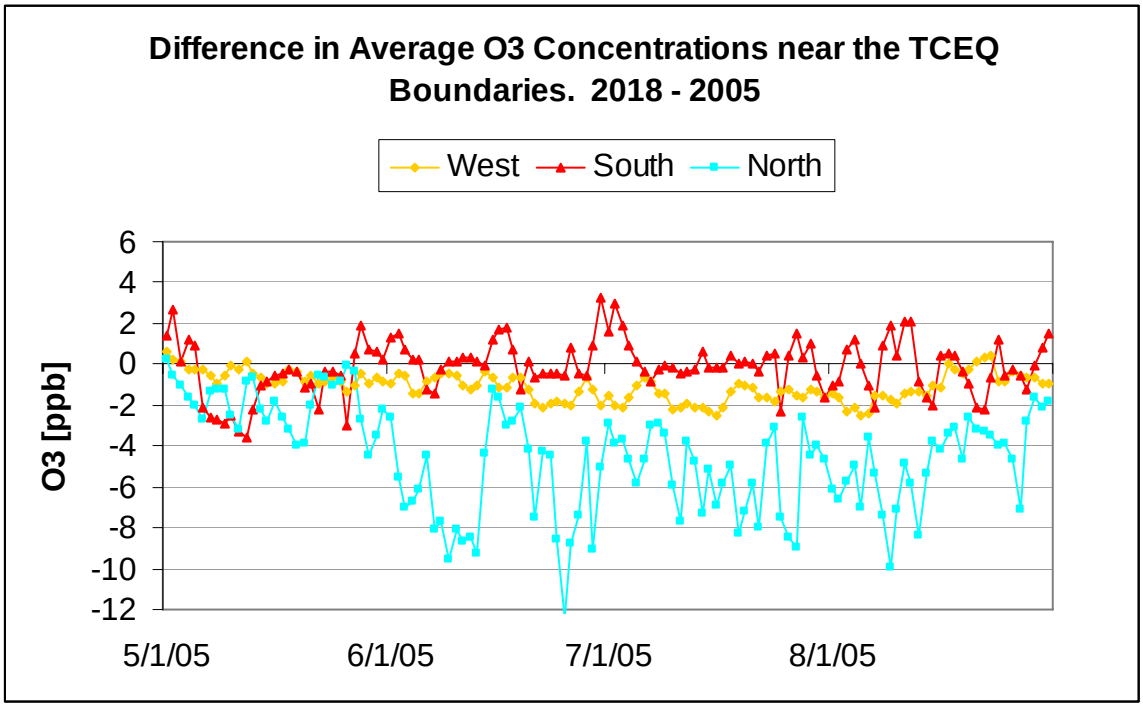

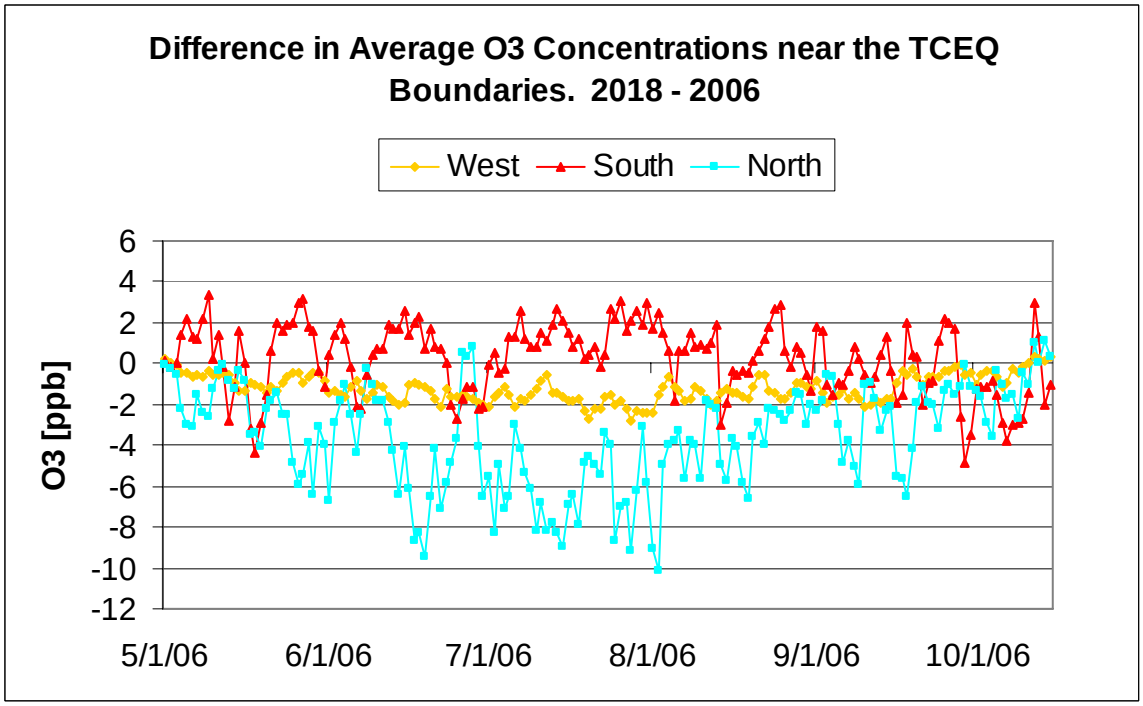

Figure ES-2. Time series of differences in daily ozone at monitoring sites near the boundaries of the TCEQ 36 km domain between 2005 and 2018 (top) and 2006 and 2018 (bottom).

1. INTRODUCTION

Biomass burning can emit substantial amounts of particulate matter, NOx, and VOCs, which have the potential to significantly increase ozone production downwind of each fire. An analysis of fires in the western US during the summers of 1989 to 2004 showed that a typical fire season increased ozone an average of 3.5 ppb across the entire western US during the summer months; the largest fire season enhanced summer ozone by 8.8 ppb (Jaffe, 2008).

The TCEQ 36 km modeling domain excludes the western US along with most of Mexico and Canada. To address fire emissions that could be transported into the TCEQ domain, fire emissions must be represented in the lateral boundary conditions for the TCEQ domain. This report documents preparation of CAMx-ready fire emission inventories using EPS3.

TCEQ is conducting ozone modeling for five episodes in the summers of 2005 and 2006. TCEQ domain boundary conditions were developed by performing CAMx simulations on a continental-scale 36 km domain developed by several Regional Planning Organizations (RPOs). Boundary conditions for the continental scale RPO grid were, in turn, extracted from two global models. Modeling was performed for base years (2005 and 2006) and for a future year (2018).

Studies show that biomass burning emissions derived from satellite data can provide realistic spatial and temporal patterns that can be incorporated into air quality models (Wiedinmyer, 2006; Zhang, 2008). Date-specific satellite-derived fire emissions obtained from Christine Wiedinmyer at the National Center for Atmospheric Research (NCAR; Wiedinmyer, 2006) were processed for the RPO 36 km domain, which covers the entire continental US, including all of the TCEQ domain, and large portions of Canada and Mexico. The date specific fire emissions were used for base year (2005 and 2006) modeling. Boundary conditions for the TCEQ modeling domain were then extracted from CAMx outputs of the larger RPO domain to incorporate fire emissions outside of TCEQ's domain.

The CENRAP Typical 02g inventory, which represents a multi-year average of fire emissions, was also formatted and processed through EPS3. The typical fires dataset was processed for the RPO domain and used for future year (2018) modeling. The typical fire emissions also were processed for the TCEQ domain to enable TCEQ to account for fires within the domain.

New EPS3 modules were developed specifically to handle point source fire emissions – PREFIR and PSTFIR. These new modules allow each fire point source to be distributed into multiple vertical layers to better represent each fire plume. Details of the two sets of fire emissions and the EPS3 modules developed for this study, including descriptions of the chemical speciation for fire emissions, temporal allocations, and new grid surrogates, can be found in Section 2.

A discussion of the 2005 and 2006 CAMx modeling of the RPO domain with the NCAR fire emissions can be found in Section 3. CAMx was run with two sets of RPO domain boundary conditions extracted from two global models – GEOS-Chem and MOZART. An evaluation of surface ozone using ozone monitoring sites from EPA's Air Quality System (AQS) located near the TCEQ 36 km boundaries compares the impacts between GEOS-Chem and MOZART.

Section 4 describes the 2018 future year modeling of the RPO domain, which included the typical fire inventory. Results were compared to the base year ozone near the TCEQ lateral boundaries to evaluate changes between the base and future years.

2. DEVELOPMENT OF FIRE EMISSIONS

Two sets of fire emissions were processed into EPS3 inputs for the RPO domain for two time periods – May 1 to September 1, 2005, and May 1 to October 16, 2006. One set consisted of date-specific fire emissions from The National Center for Atmospheric Research (NCAR); the other set was based on the typical fires from the CENRAP 02g inventory. The typical fire inventory was also formatted for EPS3 in the TCEQ projection.

The fire inputs were run through EPS3 to generate CAMx-ready fire emissions. Two new EPS3 modules were developed specifically to handle point source fire emissions – PREFIR and PSTFIR. These new modules allow each fire point source to be distributed into multiple vertical layers to better represent each fire plume.

2.1. NCAR EPISODIC FIRE EMISSIONS

The NCAR satellite-derived fire emissions data for 2005 and 2006 were obtained from Christine Wiedinmyer at ftp://acd.ucar.edu/user/christin/FIRE/Emissions (Wiedinmyer, 2006). Daily emissions were available for most of North and Central America using version 2 of the NCAR fire emissions model. Each record consisted of location (latitude and longitude), Julian date, acreage burned, biomass burned (fuel loading), and emission estimates. The acreage burned was set to 1 km^2 in almost every record, representing the size of each satellite pixel. The pollutants included CO, PM10, PM25, NOx, NH3, VOC, SO2, Hg, CH4, HCN, and CH3CN; the latter three species were available only in 2006.

Each record was treated as a point source. A plume profile was calculated for each point in order to distribute the emissions vertically using the methodology outlined in the WRAP 2002 Phase II report (WRAP, 2005). In this report, fires were assigned to one of five fire size classes. Three plume parameters – the top and bottom of the plume and the fraction of emissions in layer 1 – could be computed from tables of buoyancy efficiencies and maximum top and bottom plume heights, which are functions of the fire size class and/or hour of the day.

The diurnal profiles, parameters, and equations needed to compute the plume attributes were obtained from the WRAP report and were incorporated into the PSTFIR routine in EPS3. The only variable not directly available from the NCAR dataset that needed to be passed into EPS3 was the fire size.

In the WRAP report, fire sizes were classed in terms of virtual acres, which are estimated from the equation below:

$$Acreage_{virtual} = Acreage_{actual} * \sqrt{FuelLoading / Normalizer}$$

WRAP normalized wildfires to 13.8 tons per acre (tpa) and prescribed fires to 5.0 tpa. The five fire classes are shown in Table 2-1. All points were treated as wildfires. Any point within 5 km of another point was assumed to be part of the same fire event. The virtual area for each fire event was set to the sum of the virtual areas from the cluster of points defining the fire event.

Table 2-1. Fire classes used by WRAP.

Fire Class	MinVirtual Area [acres]	Max Virtual Area [acres]
1	>= 0	<10
2	10	100
3	100	1000
4	1000	5000
5	5000	

Figure 2-1 compares the distribution of all fire points in June and July, 2006 (18,000 points) into the 5 fire classes before grouping (the individual point sources) and after grouping fires together. Before grouping, 77% of all fire points were assigned to class 3 (100 to 1000 virtual acres, or 0.4 to 4.0 km^2, which include the satellite-defined actual fire size of 1.0 km^2); most other points were in class 2 (10 to 100 virtual acres). After grouping points within 5 km of one another, more points were assigned to classes 4 and 5, but class 3 still contained the most number of fire points.

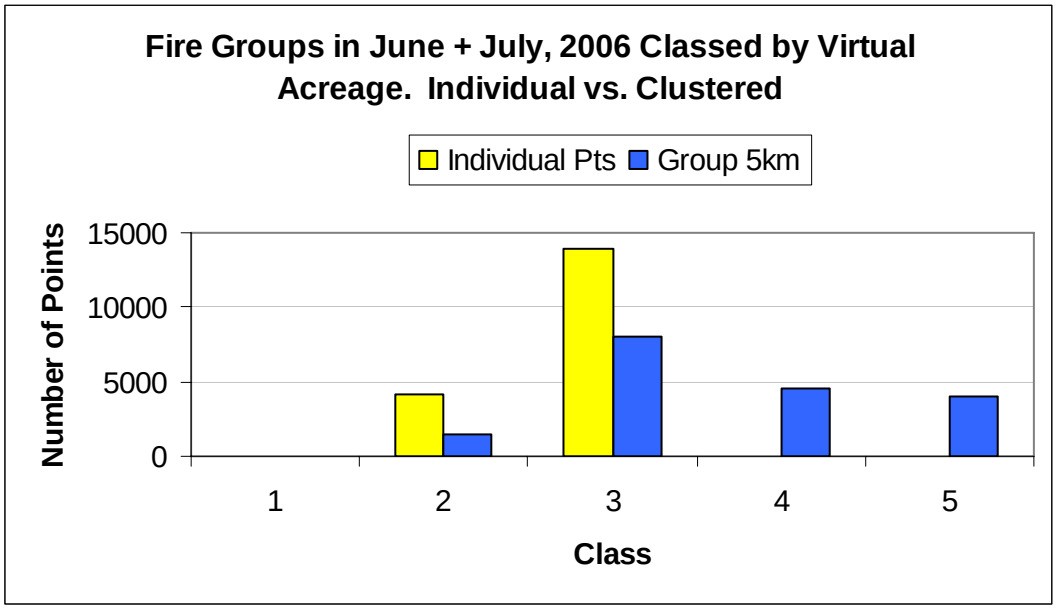

Figure 2-1. Fire point distribution before and after grouping points within 5 km of one another.

A sensitivity test examined the class distribution when the maximum grouping distance between fire points was reduced from 5 km to 3 km. Figure 2-2 shows the number of fire points in the five classes when the grouping distance was 5 km (blue) and 3 km (pink). The class distribution was not highly sensitive to changes in the maximum distance defined in grouping points.

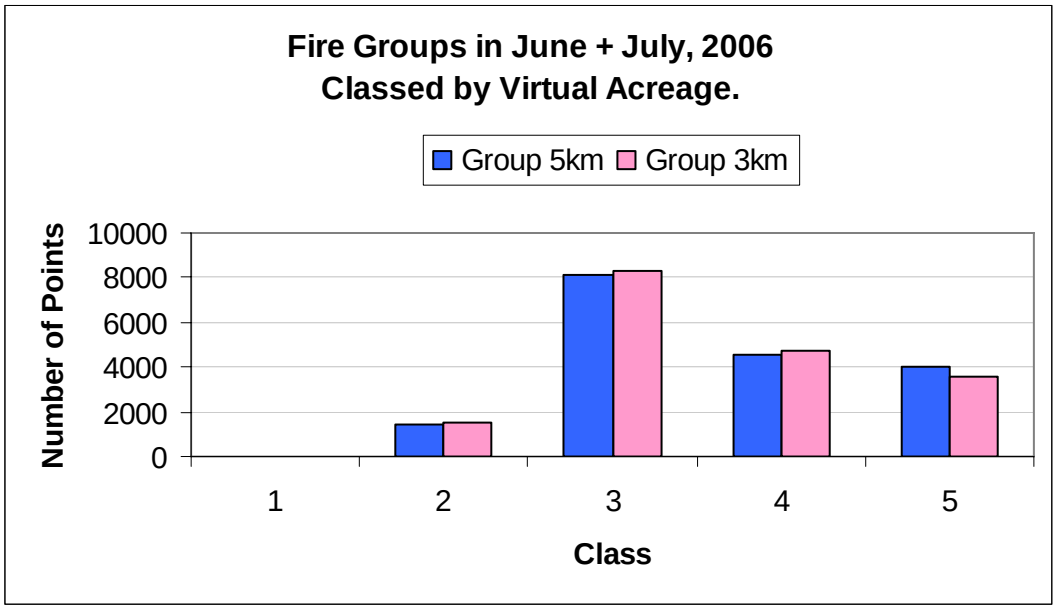

Figure 2-2. Fire point distribution when the maximum grouping distance is 5 km and 3 km.

A second sensitivity test examined the fire class distribution when the area burned was reduced by 50% for points not clustered to any other point. In this case we assumed that for small fires (non-clustered points), the actual fire size would not cover the full 1 km^2 satellite pixel while larger fires (clustered points) could be burning in the entire 1 km^2 area. These class distributions were also compared to the daily classed PM2.5 emissions of each fire point, whose emissions were also summed together when considered part of the same fire cluster. The PM2.5 class bins used a comparable range of bins in a logarithmic scale as listed in Table 2-2, and could be an alternative method to classify the magnitude of the fires.

Table 2-2. Comparison of virtual area and PM2.5 emission bins.

Class	Virtual Area (Max Value in Bin, Acres)	PM2.5 Emissions (Max Value in Bin, kg/day)
1	10	1,000
2	100	10,000
3	1,000	100,000
4	5,000	500,000
5	>5,000	>500,000

Bar charts of class distributions from the three methods are shown in Figure 2-3 using a 5 km maximum aggregation distance. When the fire area was reduced by 50% for the smaller fires (individual points), denoted by the green bars in Figure 2-3, approximately 1500 fire points migrated from class 3 to class 2 while the other classes showed little change.

The fire distribution of the five classes sorted by PM2.5 emissions and by virtual area when the burn area was reduced 50% for non-clustered points had similar profiles, suggesting that there should be a reduction in the 1 km^2 size for these individual points. Figure 2-4 shows a scatterplot of each fire point comparing the daily PM2.5 emissions to the virtual area with the 50% reduction for individual points; both axes are on a logarithmic scale. The pink lines represent the fire class bins. The plot shows a strong correlation between the two variables.

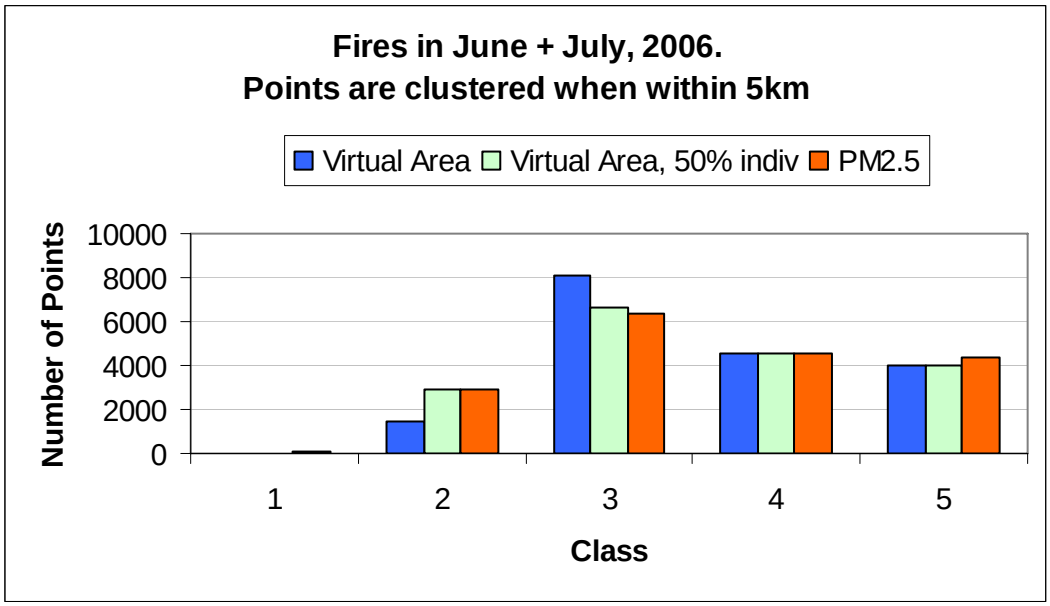

Figure 2-3. Comparison of fire classes sorted by virtual acreage, virtual acreage cut by 50% for individual fire points, and daily PM2.5 emissions.

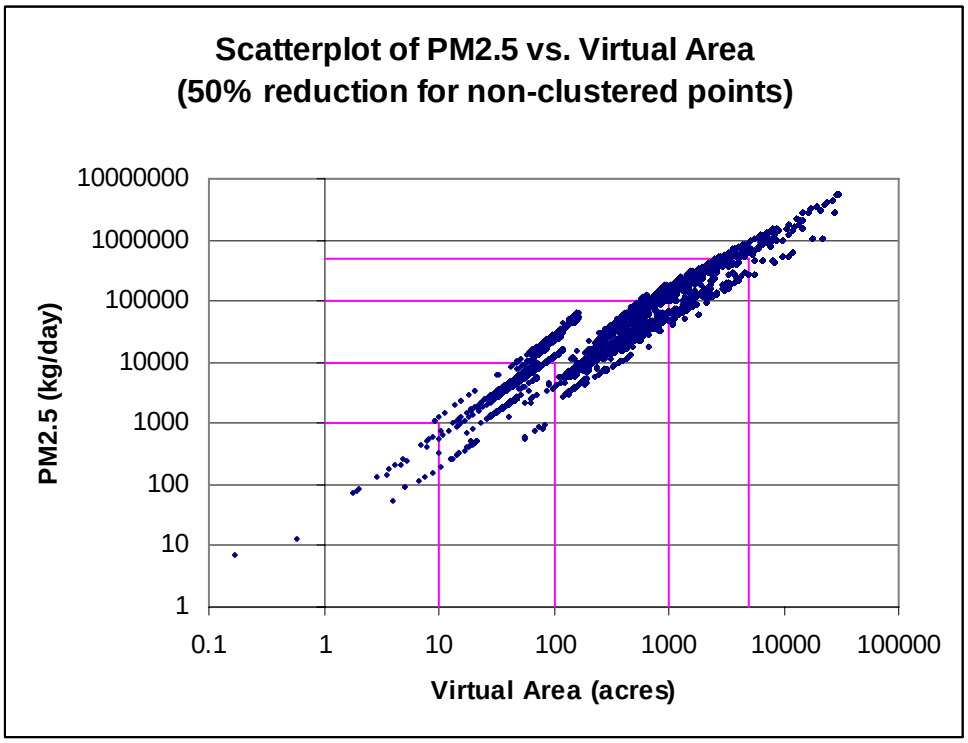

Figure 2-4. Scatterplot of fire points comparing daily PM2.5 emissions to the virtual area.

Table 2-3 summarizes the PM2.5 fire emissions in the RPO CAMx domain for June and July, 2006. The number of large fires (group containing more than one point when using the 5 km threshold) is also listed, accounting for an average of 70% of all points for each date.

Table 2-3. Number of fire points and total PM2.5 emissions for June and July.

Date	PM2.5 tons/day	Total Number of Points	Number of Points in Clusters	Date	PM2.5 tons/day	Total Number of Points	Number of Points in Clusters
1-Jun-06	5978	196	113	1-Jul-06	2967	164	119
2-Jun-06	3438	174	76	2-Jul-06	2137	98	34
3-Jun-06	2941	140	72	3-Jul-06	1777	108	55
4-Jun-06	2491	138	95	4-Jul-06	3105	149	64
5-Jun-06	5706	236	122	5-Jul-06	2343	111	53
6-Jun-06	6171	227	134	6-Jul-06	4134	146	89
7-Jun-06	4995	213	117	7-Jul-06	1520	90	36
8-Jun-06	5479	214	114	8-Jul-06	2052	100	55
9-Jun-06	4936	202	125	9-Jul-06	585	45	22
10-Jun-06	8860	374	203	10-Jul-06	4207	139	93
11-Jun-06	5345	200	135	11-Jul-06	3798	181	139
12-Jun-06	7780	293	213	12-Jul-06	9026	439	342
13-Jun-06	6956	287	177	13-Jul-06	9872	722	633
14-Jun-06	11307	426	301	14-Jul-06	10392	673	585
15-Jun-06	8483	373	268	15-Jul-06	7521	464	391
16-Jun-06	15026	485	384	16-Jul-06	10873	639	534
17-Jun-06	6407	216	131	17-Jul-06	9651	432	304
18-Jun-06	4869	215	145	18-Jul-06	11109	602	484
19-Jun-06	10380	340	252	19-Jul-06	7222	375	255
20-Jun-06	9634	348	252	20-Jul-06	4671	206	106
21-Jun-06	11446	383	293	21-Jul-06	5446	242	181
22-Jun-06	3383	146	72	22-Jul-06	3403	181	120
23-Jun-06	4853	210	136	23-Jul-06	3093	175	125
24-Jun-06	3407	146	75	24-Jul-06	6716	266	197
25-Jun-06	6523	257	223	25-Jul-06	6776	278	219
26-Jun-06	3196	129	101	26-Jul-06	14580	508	467
27-Jun-06	1457	89	66	27-Jul-06	19725	631	571
28-Jun-06	5075	231	152	28-Jul-06	22072	923	863
29-Jun-06	5428	217	139	29-Jul-06	30254	862	779
30-Jun-06	3604	157	70	30-Jul-06	19093	611	542
				31-Jul-06	10694	346	256

The NCAR fire emissions were reformatted into the new EPS3 input format for point source fires. Each record includes the FIPS code, SCC, optional IDs, time, location, virtual area, and emissions rate for each species. The format of the new input file is shown in Table 2-4. The NCAR data listed country and state data, but not county-level. The FIPS codes within the US consisted of the state FIPS followed by "000". Fires outside the US used a two letter country identifier followed by the state or province number, if available. The SCC was set to 2810001000 (wildfires) for all records. The virtual area, which will be used in PSTFIR to estimate the vertical extent of the fire plumes for each hour of the day, was reduced 50 % for individual points, and was set to the sum of all virtual acreages from all points within a fire cluster using the 5 km distance threshold.

Table 2-4. EPS3 input format for point source fire emissions.

Column Beginning	Column End	Type	Description
1	5	C	FIPS State/county code
7	16	C	Source classification code (SCC)
18	27	C	Fire ID
29	38	C	Cluster ID (optional)
40	41	C	Period type S = Specified interval
43	50	I	Beginning period interval date/time; time is in military format (YYMMDDHH)
52	59	I	Ending period interval date/time
61	70	R	Latitude or easting coordinate (km)
72	81	R	Longitude or northing coordinate (km)
83	84	I	UTM zone. List value only if coordinates are in UTM
86	93	R	Virtual area of fire (acres)
95	99	I	Pollutant code
101	110	R	Emissions of pollutant (tons/period)
112+			Miscellaneous comments

2.2. TYPICAL FIRES

EPS3 inputs were also prepared for a typical fire emissions inventory, which represents a multi-year average of fire emissions that can be incorporated into base and future year modeling. The typical fire inventory was obtained from the CENRAP 2002 Typical 02g dataset in SMOKE IDA format and consisted of both area and point sources. Table 2-5 lists the SMOKE-formatted area and point source typical fire files in each region.

All fires in the WRAP states were elevated; fires in the CENRAP and VISTAS states contained both area and point sources. Fires in all other areas were reported as area sources. CENRAP assigned a fire as a point source only when the location, time, and size of fire were known. The CENRAP agricultural burning inventory was the most detailed among all the RPOs, listing emission estimates and temporal profiles for many specific crops, including alfalfa, barley, red bean, corn, grasses, hay, oats, pea, rice, sorghum, sugarcane, and wheat. Details on the development of the fire inventory can be found in *Research and Development of Planned Burning Emission Inventories for the Central States Regional Air Planning Association* (CENRAP, 2004).

There were no records of agricultural burning in the typical fire inventory from the MRPO states or in Canada.

Table 2-5. List of the typical fire files in SMOKE-format for area sources (top) and point sources (bottom) for each region.

Region	Anthropogenic Area Sources
CENRAP	Arfinv_anthro_cenrap2002_081705.ida
WRAP	--
VISTAS	Arfinv_anthro_vistas2002_TypicalFires_no2610000_112704.ida
MRPO	Arfinv_anthro_mrpok_2002_20jun2006.ida
MANE-VU	Arfinv_anthro_mane-vu2002_011705.ida
Canada	Arfinv_anthro_CANADA2000_v2.ida
Mexico	Arfinv_anthro_Mexico99phase3_border_20051027v4.ida
Mexico(2)	Arfinv_anthro_Mexico99phase3_interior_ERG_Oct06.ida
Region	**Wildfire Area Sources**
CENRAP	arfinv_wf_cenrap2002_081705.ida
WRAP	--
VISTAS	arfinv_wf_vistas2002_TypicalFires_No2610000_112704.ida
MRPO	arfinv_wf_mrpok_2002_20jun2006.ida
MANE-VU	arfinv_wf_mane-vu2002_011705.ida
Canada	arfinv_wf_CANADA2000_v2.ida
Mexico	arfinv_wf_Mexico99phase3_border_20051027v4.ida
Mexico(2)	arfinv_wf_Mexico99phase3_interior_ERG_Oct06.ida
Region	**Point Sources**
CENRAP	Ptinv_2002CENRAP_ptfires_mon$MM.ida
WRAP (prescribed)	Ptinv_200510211029_wrap2002_rx_base.mon$MM.ida
WRAP (wildland fire use)	Ptinv_200510211022_wrap2002_wfu_base.mon$MM.ida
WRAP (agriculture fires)	Ptinv_200507011516_wrap2002_agf_base.mon$MM.ida
WRAP (non-federal prescribed rangeland burn)	Ptinv_200504051315_wrap2002_nfr.mon$MM.ida
WRAP (wildfires)	Ptinv_200510210936_wrap2002_wild_base.mon$mm.ida
VISTAS	Ptinv_agfires_$MM_vistas.ida
MRPO	--
MANE_VU	--
Canada	--
Mexico	--

where $MM = month number

Typical Fire Point Sources

Elevated point sources were available from the WRAP, CENRAP, and VISTAS RPOs. A perl program, ida2afs_fire.prl, was developed to reformat the SMOKE inputs to EPS3 fire inputs. The SMOKE point source inputs consist of three files: PTINV, which includes point parameters such as the FIPS, SCC, and location (latitude and longitude); PTDAY, which contains the date-specific daily emission rate of each point source, and PTHOUR, which contains the plume parameters (fraction of emissions that should go into layer 1, and the heights of the plume top and bottom) for each hour of the day.

EPS3 will compute hourly fire plume characteristics based on the methodology in the WRAP report; instead of carrying 72 variables for each point source through EPS3, the hourly plume profiles could be recomputed in the new PSTFIR module by simply passing the virtual fire size. The equations to compute the fraction in layer 1 and the plume top and bottom were backtracked to determine the fire size class; then, an appropriate virtual fire size was assigned to the point. No clustering of points was performed.

Within each RPO, all fire point sources had the same three or four diurnal plume profiles for plume top, plume bottom, and fraction of emissions in layer 1. There were no fires in Class 5. The plume characteristics in the CENRAP states were based on parameters found in the WRAP Phase I report (WRAP, 2004). The WRAP fires matched the profiles found in the WRAP Fire Emissions Phase II report (WRAP, 2005), where the plume bottoms in Fire Classes 4 and 5 were revised lower, and where the fraction of emissions in layer 1 was no longer scaled to the depth of the first layer.

VISTAS' fire plume profiles had much lower peak plume tops and bottoms than either CENRAP or WRAP, but the profiles of the fraction of emissions in layer 1 equaled that of WRAP. The latter was used to classify the VISTAS fire point sources into the appropriate fire class. The left and right sides of Figure 2-5 compare the diurnal profiles of the plume top and plume bottom in Fire Class 4 (fires between 1000 and 5000 acres) between CENRAP, WRAP, and VISTAS.

All fires would later be processed with the plume profiles defined by WRAP. Typical point source fire emission inventories were generated in EPS3 fire format for both the RPO domain and for the TCEQ domain. Emissions were processed for NOx, VOC, CO, SO2, NH3, PM2.5, and PM10. Duplicate records in the SMOKE inputs were also repeated in the EPS3 inputs since SMOKE would sum these emissions together; an extension (_2, _3, etc) was attached to the fire ID of duplicate records.

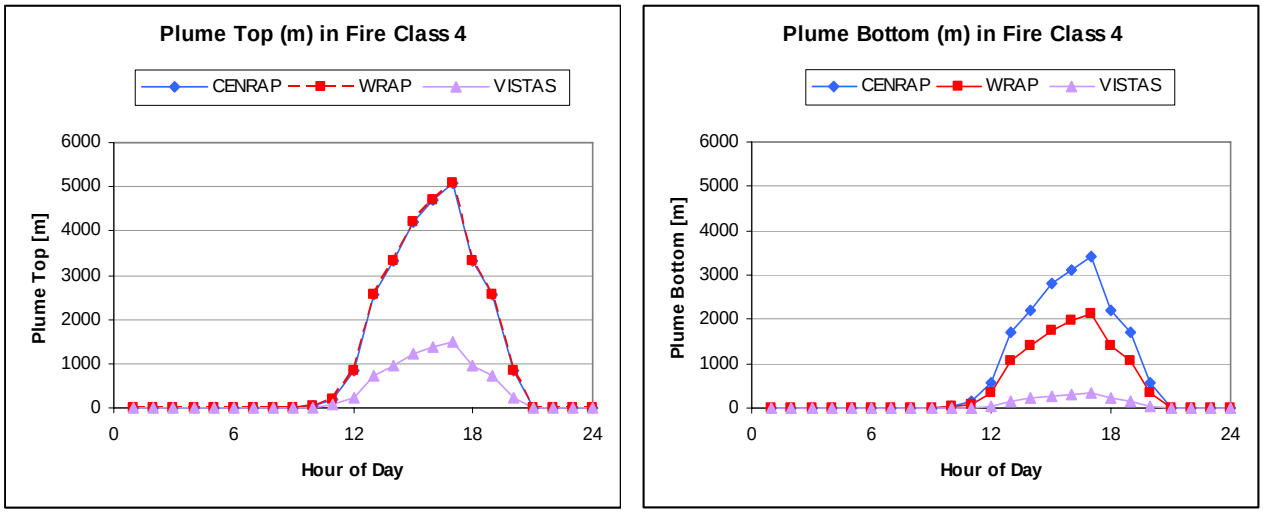

Figure 2-5. Diurnal profiles of Fire Class 4 plume top and plume bottom in the CENRAP, WRAP, and VISTAS typical fire inventory.

Typical Fire Area Sources

The SMOKE area source files (ARINV files in IDA format), which contain annual and countywide-total fire emissions, were reformatted into the standard EPS3 AMS format, putting all emissions into layer 1 of the modeling domain. Ideally, fire emissions should be spread into layers aloft, but the lack of information regarding the fire size and specific location limited our capabilities of defining plume profiles. All fire emissions from WRAP were in the elevated point source inventory, so there was no WRAP area source fire file.

Both elevated and area source typical fires were formatted into EPS3 inputs for both the entire RPO domain, and for the TCEQ domain.

2.3. PROCESSING FIRE EMISSIONS USING EPS3

New EPS3 modules were developed to improve the vertical distribution of fire point sources. For location specific fire sources, the EPS3 processing stream executed the following modules:

PREFIR → SPCEMS → TMPRL → PSTFIR → PIGEMS

For area sources, the standard area source EPS3 processing stream was applied.

PREAM → SPCEMS → TMPRL → GRDEM

PREFIR

The new PREFIR module reads in point source fire emissions in the fire input format described in Table 2-4 and outputs data in the EMBR format. On a few dates, the number of fire points exceeded 1000 points with 8 pollutants per point. In order to reduce the number of points, fire points of the same fire class, FIPS, and SCC were combined when located in the same grid cell, which was set to a 4 km resolution for this application. All points were shifted to the grid cell center.

PREAM

The PREAM module reads in county-total area source emissions in the AMS format and reformats the data to the EMBR format. All emissions remain in the surface level.

SPCEMS

SPCEMS performs similar duties as CHMSPL, which speciates a criteria pollutant into model-ready species, but allows the speciation of multiple criteria pollutants. SPCEMS also allows computation between species, including the calculation of coarse PM (CPRM), computed from the difference of PM10 and PM2.5.

Chemical speciation profiles in this task were derived from a recent study on tropical biomass burning (Karl et al., 2007). The study integrated laboratory experiments and field measurements conducted as part of the TROFFEE (Tropical Fire and Forest Emissions Experiment) campaign. The combination of laboratory and field measurements makes it possible to report many compounds previously not quantified in the field and therefore not included in previous studies.

All fire VOC emissions were converted to TOG and split into CB05 species. The VOC to TOG conversion factor for all point and area source fires was 1.04272872. Emissions were allocated to CB05 species using the factors in Table 2-6, where

$$Emis_{CB05} = Emis_{TOG} * SplitFactor / Divisor * 16 \frac{g}{mol} * \#Carbons$$

Table 2-6. Factors used to convert TOG to CB05 species for fire emissions.

Criteria Pollutant	CB05 Species	Split Factor	Divisor [mol/g]	# Carbons
TOG	ALD2	0.1519	43.5932	2
TOG	ALDX	0.0622	37.1144	2
TOG	FORM	0.0619	29.2445	1
TOG	ISOP	0.024	68.117	5
TOG	MEOH	0.1766	32.0419	1
TOG	OLE	0.0383	36.9936	2
TOG	PAR	0.2334	22.0391	1
TOG	TOL	0.0285	92.2464	7
TOG	UNR	0.2091	22.8743	1
TOG	XYL	0.014	106.165	8

PM2.5 was speciated using split factors extracted from the CENRAP 2018g inventory files:

- Gspro.cmaq.cb4p25.072606.txt
- Gsref.cmaq.cb4p25.072606.txt.

PM2.5 from all wildfires, including all fire sources from the NCAR inventory, were mostly split into primary organics (POA) (77%) and primary elemental carbon (PEC) (16%), as shown in Figure 2-6. The default (non-CENRAP) profiles for prescribed and agricultural burning also allocated most PM2.5 emissions to POA; in the CENRAP states, more was allocated to FPRM compared to the non-CENRAP states and less went to POA.

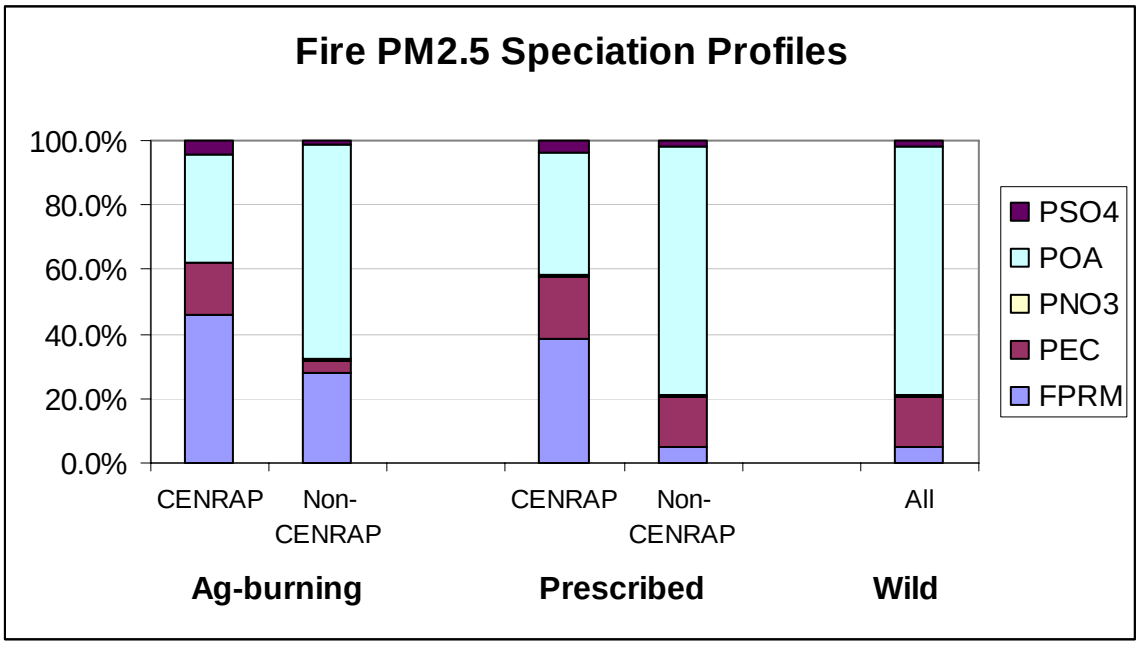

Figure 2-6. PM2.5 speciation profiles.

TMPRL

The TMPRL module allocates emissions by month, day of week, and diurnally and adjusts the hourly profiles to the appropriate time zone, based on a record's SCC and FIPS.

The NCAR episodic emissions were date specific and could not be attributed to a certain type of fire, so the default diurnal profile found in the WRAP Phase II report was used for all fires (WRAP, 2005). Figure 2-7 displays the diurnal allocation of the daily NCAR fire emissions. Emissions peaked between 2PM and 4PM and were relatively low at night and early morning.

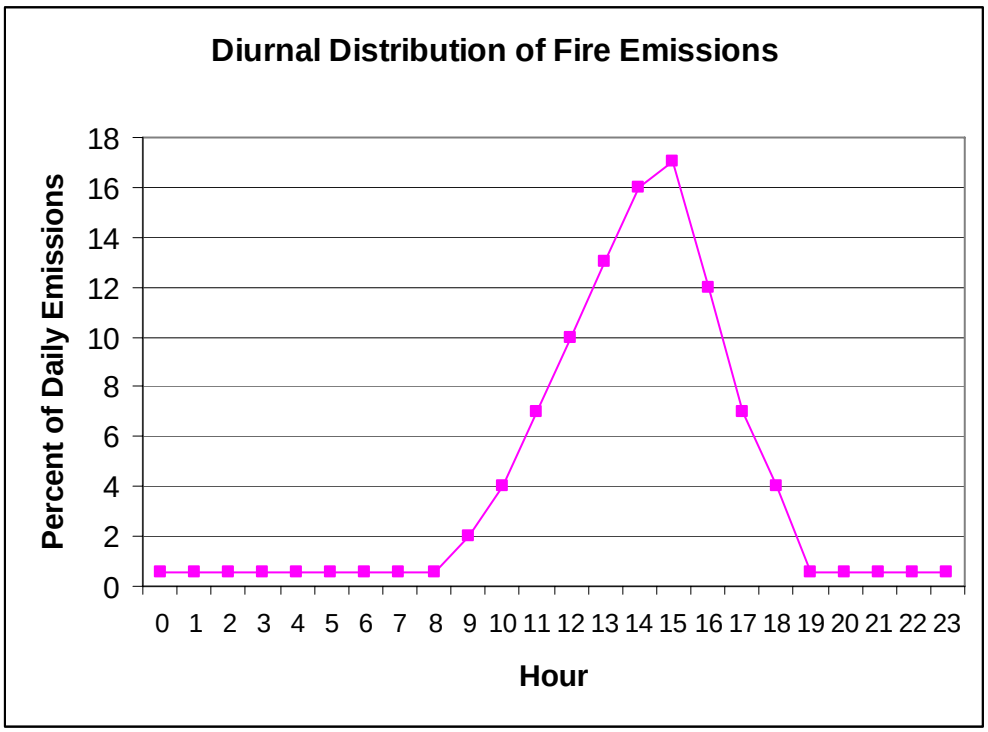

Figure 2-7. Standard diurnal distribution of daily fire emissions.

Inputs to the area source typical fires contained annual emissions. The detailed agricultural burning emissions inventory in the CENRAP states were coupled with monthly, weekly, and diurnal allocations for specific crops in each CENRAP state, as was applied to the WRAP Plan 02d inventory. The temporal allocations were extracted from these WRAP files:

amtpro.m3.111805.WRAP_Plan02.txt
amtref.m3.111805.WRAP_Plan02.txt

The monthly temporal profiles helped differentiate profiles in northern states like Minnesota and Iowa, where peak agricultural burning occurred later in the spring than in most other CENRAP states. Figure 2-8 illustrates the monthly allocation for corn field burning in two southern states (Texas and Louisiana), shown in shades of red, and in two northern states (Minnesota and Iowa), denoted in blue, showing a time lag in both spring and fall. The EPA default agricultural burning profile for all crops is depicted in grey, showing a peak in spring; the default profile underestimates the level of fires set to corn fields in the fall in all states. The detailed temporal profiles also distinguished the burning of winter wheat in Arkansas and sugarcane in Louisiana, both which peak in the fall.

An updated version of the WRAP temporal profile list, amtref.m3.092706.WRAP_Plan02.txt, included monthly profiles for agricultural field burning in four VISTAS states -- Alabama, Florida, Georgia, and South Carolina; the other VISTAS states used the average monthly profile

from these four states. The CENRAP agricultural burning records were not included in this file. In this project, both sets of temporal profiles for crop burning in the CENRAP and VISTAS states were applied.

The VISTAS typical fire inventory did not differentiate the burning of different crop types except wheat fields in North Carolina. Peak crop burning in each VISTAS state occurred in February and March, except Florida, where the most agricultural burning took place in January. Figure 2-9 displays the monthly allocation of the annual emissions for each VISTAS state. The monthly EPA default profile was also included, showing peak crop burning in the VISTAS states months after the default profile. VISTAS, CENRAP, and EPA default monthly profiles all allocated little in the summer months.

Agricultural fires in MANE-VU and Mexico also did not distinguish crop types. No specific profiles were available, so the EPA default monthly profile was used in these regions. The WRAP inventory also bundled crop types together. Since all WRAP fires were listed as point sources, which list date-specific emissions, monthly profiles were not needed.

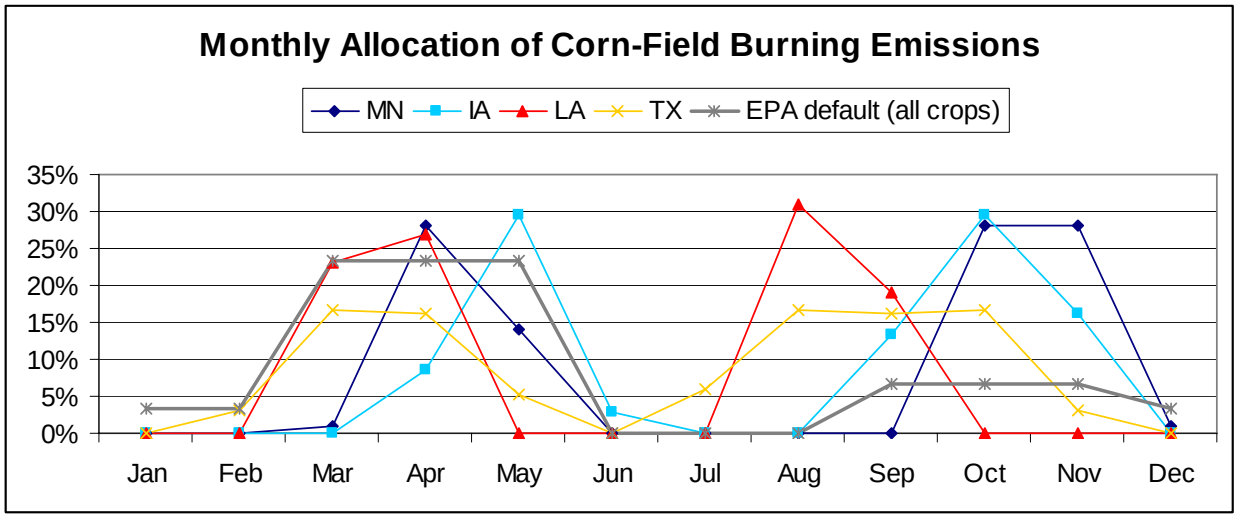

Figure 2-8. Monthly profiles of agricultural burning of corn in northern and southern CENRAP states.

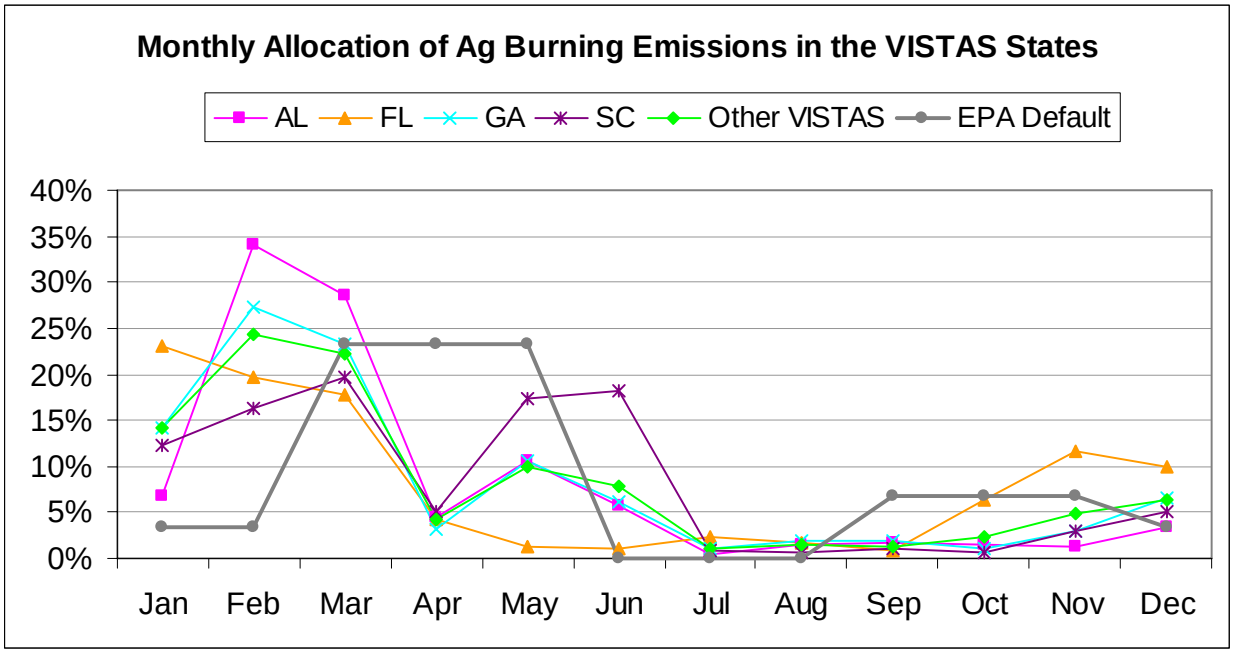

Figure 2-9. Monthly profiles of agricultural burning in VISTAS states.

The day of week profiles for agricultural burning for all CENRAP states were the same for all crops within a state, but varied from state to state. Figure 2-10 shows a bar chart comparing weekday and weekend day emissions allocation. All weekdays were treated the same and Saturdays were treated the same as Sundays. Most states distributed slightly more emissions to a weekday than a weekend day. The main exceptions were Iowa, which had no agricultural fires on weekends, and Minnesota and Missouri, which had slightly more crop burning allocated to the weekends.

For all area sources outside of the CENRAP states, there was no difference in the day of the week.

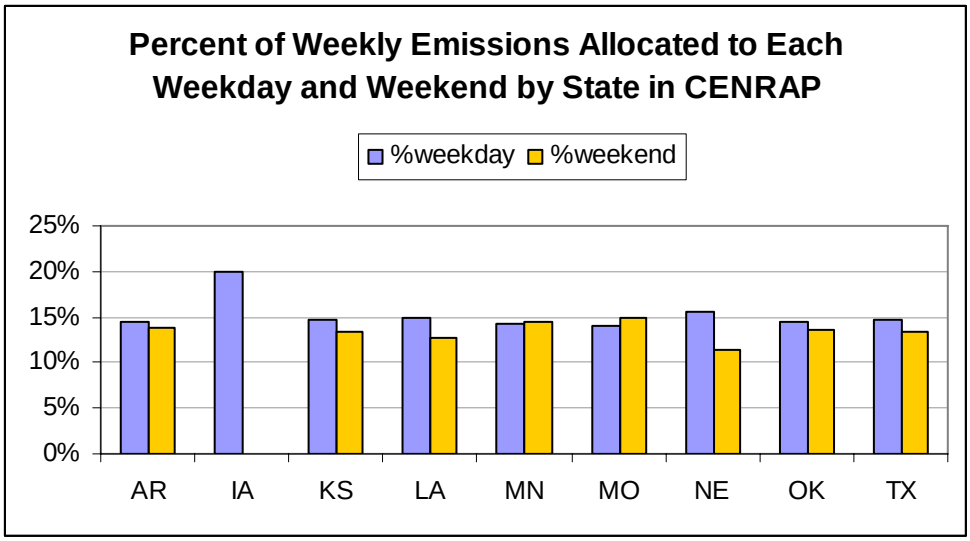

Figure 2-10. Allocation of agricultural burning emissions by day of week in the CENRAP states for all crops.

The diurnal profiles for agricultural field burning differed greatly between each RPO, as shown in Figure 2-11. The WRAP diurnal profile (and default) allocated a spike in emissions at 1 PM (17% of the daily total), with less than 1% allocated to each hour between 7PM and 9AM. The peak occurred two hours earlier than the generic profile found in the WRAP Phase II report (WRAP, 2005). CENRAP diurnal profiles were crop and state-specific, but generally showed the same pattern. Between 6AM and 6PM, the percent of daily emissions allocated to each hour was constant, varying from 5% to 9%, depending on the crop and state. During all other hours, the diurnal allocation was constant and much lower than the daytime hours; each nighttime hour was allocated no more than 3% of the daily total emissions. The average of all CENRAP profiles is displayed in Figure 2-11.

The diurnal profile for crop burning in the VISTAS region was the same for all crops and states; the profile was smoother than CENRAP, allocating 2% of the daily total to each hour at night and up to 6 % in the early afternoon.

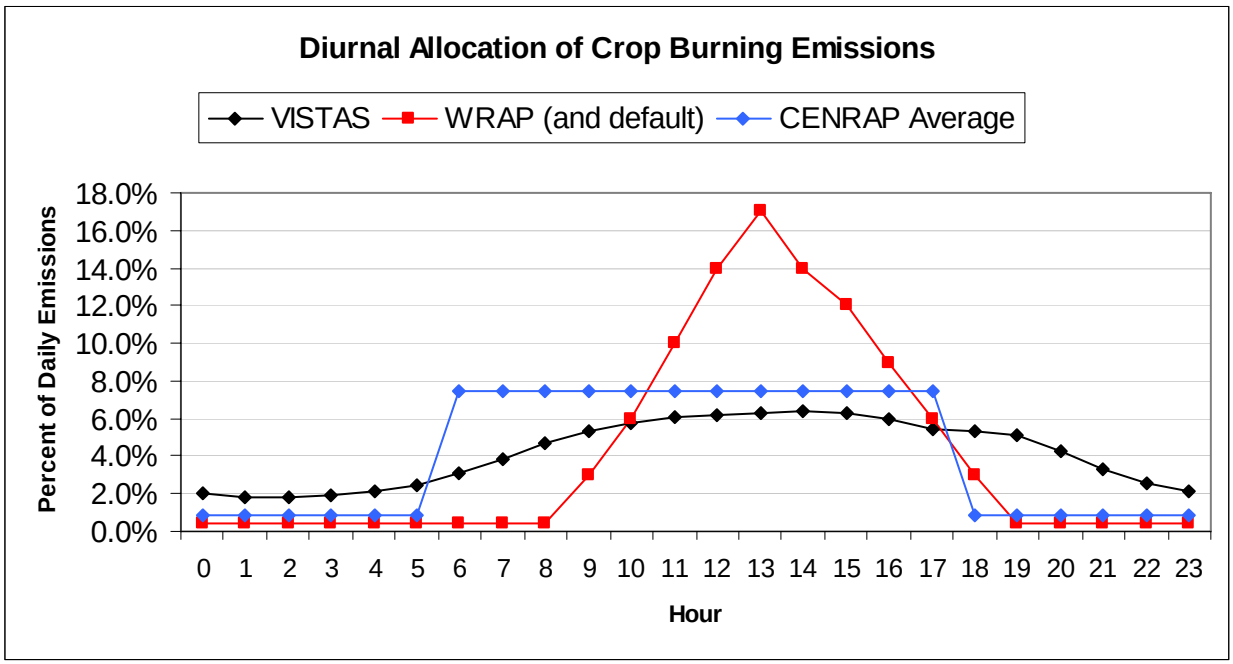

Figure 2-11. Diurnal agricultural burning profiles.

Besides agricultural burning, temporal profiles were also found for state-specific typical prescribed fires and wildfires for all 50 states. The monthly profiles differed from state to state; all days of the week were treated the same in all states. Diurnal profiles for prescribed fires allocated most emissions in the daytime; for wildfires, the allocation was more uniform, but slightly higher in the daytime. Figure 2-12 compares the diurnal profiles between wild and prescribed fires in Texas. The average profiles among the 50 states are also displayed, showing similar diurnal allocations as in Texas.

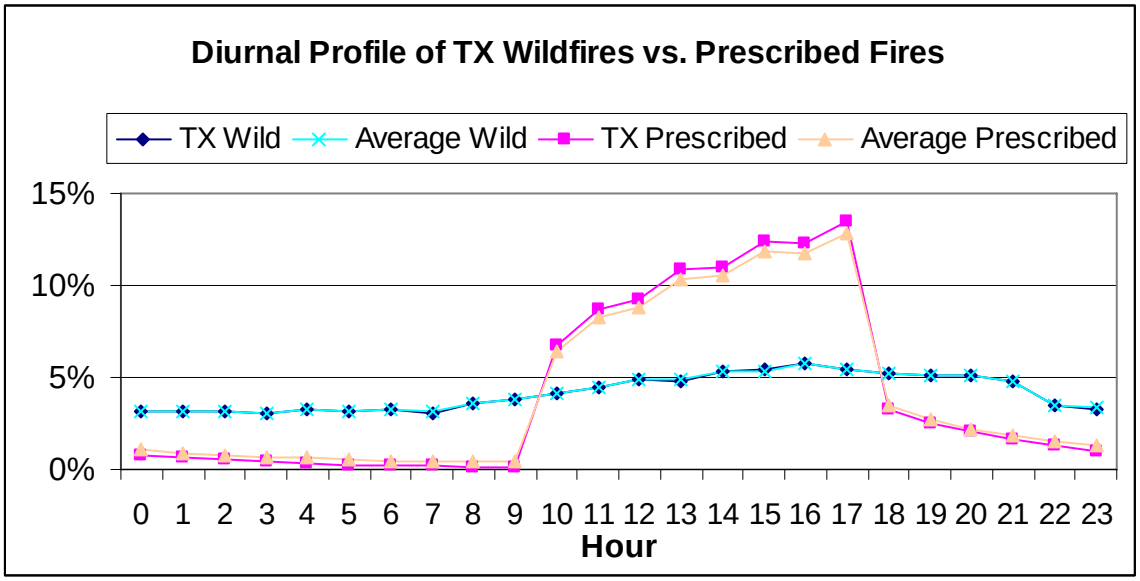

Figure 2-12. Diurnal profiles of wildfires and prescribed fires in Texas and in the US.

PSTFIR

The new PSTFIR module vertically distributes point source emissions based on the formulas found in the WRAP Phase II report (WRAP, 2005). The plume top, plume bottom, and fraction of emissions assigned to layer 1 can be computed from the fire class, determined from the virtual acreage (an input to PREFIR), and buoyancy efficiencies, which are fire size and time-of-day dependent.

The fire classes and parameters found in the WRAP Phase II report were used to compute the plume parameters for all fire point sources. Tables 2-7 and 2-8 list parameters needed for the plume calculations and the corresponding PSTFIR defaults.

The three plume parameters – top and bottom of each plume and fraction of emissions in layer 1 – can be computed for each hour as follows:

$$Ptop_{hour} = (BE_{hour})^2 * (BE_{size})^2 * Ptop_{\max}$$

$$Pbot_{hour} = (BE_{hour})^2 * (BE_{size})^2 * Pbot_{\max}$$

$$Lay1F_{hour} = 1.0 - (BE_{hour} * BE_{size}),$$

where BE_{hour} and BE_{size} are buoyancy efficiencies as a function of hour of day and fire size, respectively.

Table 2-7. Fire-related parameters as a function of fire size class.

Fire Class	1	2	3	4	5
Size (Virtual acres)	0 – 10	>= 10 to 100	>=100 to 1000	>= 1000 to 5000	> 5000
BE_{size}	0.40	0.60	0.75	0.85	0.90
$Ptop_{max}$(m)	160	2400	6400	7200	8000
$Pbot_{max}$(m)	0	900	2200	3000	3000

Table 2-8. Buoyancy efficiency as a function of hour of day.

Hour	BE_{hour}	Hour	BE_{hour}
0	0.03	12	0.70
1	0.03	13	0.80
2	0.03	14	0.90
3	0.03	15	0.95
4	0.03	16	0.99
5	0.03	17	0.80
6	0.03	18	0.70
7	0.03	19	0.40
8	0.06	20	0.06
9	0.10	21	0.03
10	0.20	22	0.03
11	0.40	23	0.03

The fraction of emissions in layer 1 was output into a gridded surface emissions file. All other emissions were output as elevated sources. Figure 2-13 displays the fraction assigned to layer 1 by hour and fire class and shows smaller fires retained more emissions in the surface layer. PSTFIR created multiple point sources as new point sources were assigned to each vertical layer that contained a part of the plume. Each new point was assigned a stack height in the middle of the layer. The negative value of the stack height was output to tell CAMx to override the plume rise calculation. Emissions were distributed to each point based on layer thickness, and were reduced accordingly when the plume spanned only part of the vertical layer.

A reference state vertical layer structure for the 19-layer RPO domain was used to allocate the fire emissions vertically. The height structure assumed a sea level pressure and temperature of 1000 mb and 300K, respectively, and a temperature lapse rate of 50K when the pressure changes by a factor of e. The layer interfaces are shown in Table 2-9.

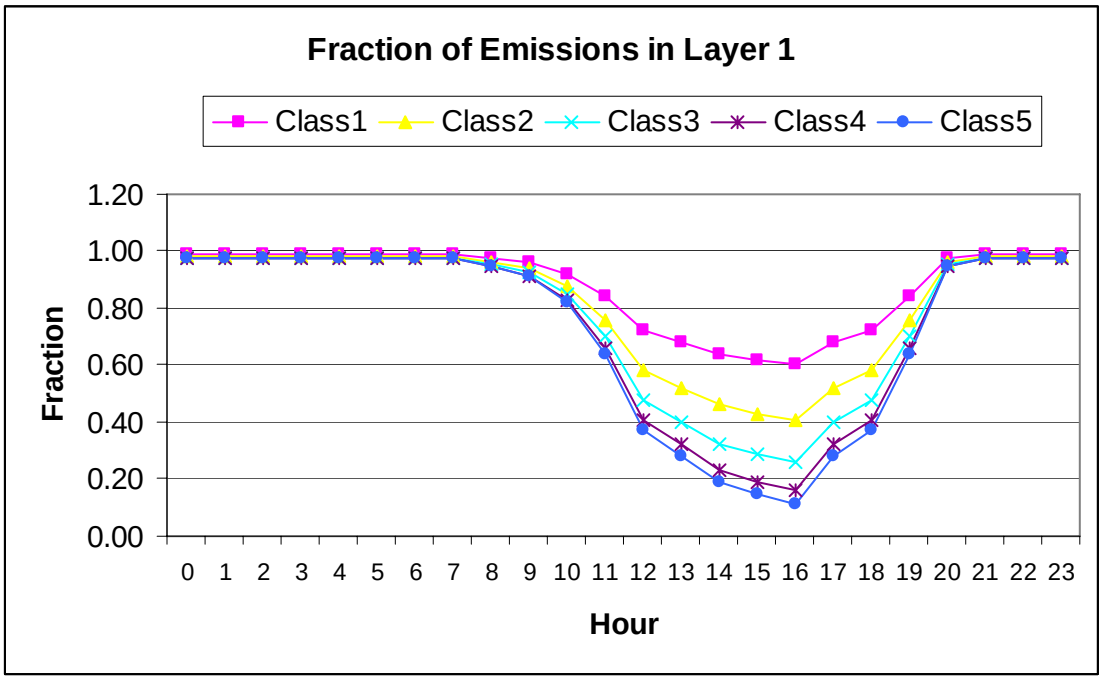

Figure 2-13. Fraction of emissions assigned to the surface emissions file by fire class.

Table 2-9. Vertical layer structure for the 19-layer RPO domain.

k	sigma	Pressure (mb)	Temperature (K)	Height (m)
19	0	100	184.87	16350.39
18	0.25	325	243.8	8950.92
17	0.45	505	265.84	5661.43
16	0.6	640	277.69	3775.65
15	0.7	730	284.26	2692.82
14	0.77	793	288.4	1998.58
13	0.82	838	291.16	1530.11
12	0.86	874	293.27	1170.1
11	0.88	892	294.29	994.69
10	0.9	910	295.28	822.19
9	0.92	928	296.26	652.5
8	0.94	946	297.22	485.53
7	0.95	955	297.7	403.03
6	0.96	964	298.17	321.18
5	0.97	973	298.63	239.96
4	0.98	982	299.09	159.36
3	0.985	986.5	299.32	119.3
2	0.99	991	299.55	79.38
1	0.995	995.5	299.77	39.62
0	1	1000	300	0

Figure 2-14 shows the layers in which emissions would be distributed for each hour and fire class based on the layer structure in Table 2-9. A bar extending from 1 to 3 means the fire emissions should be allocated into layers 2 and 3. All fire emissions in Fire Class 1 were assigned to layer 1. Fires in Class 5 were assigned emissions up to layer 18 in the mid afternoon.

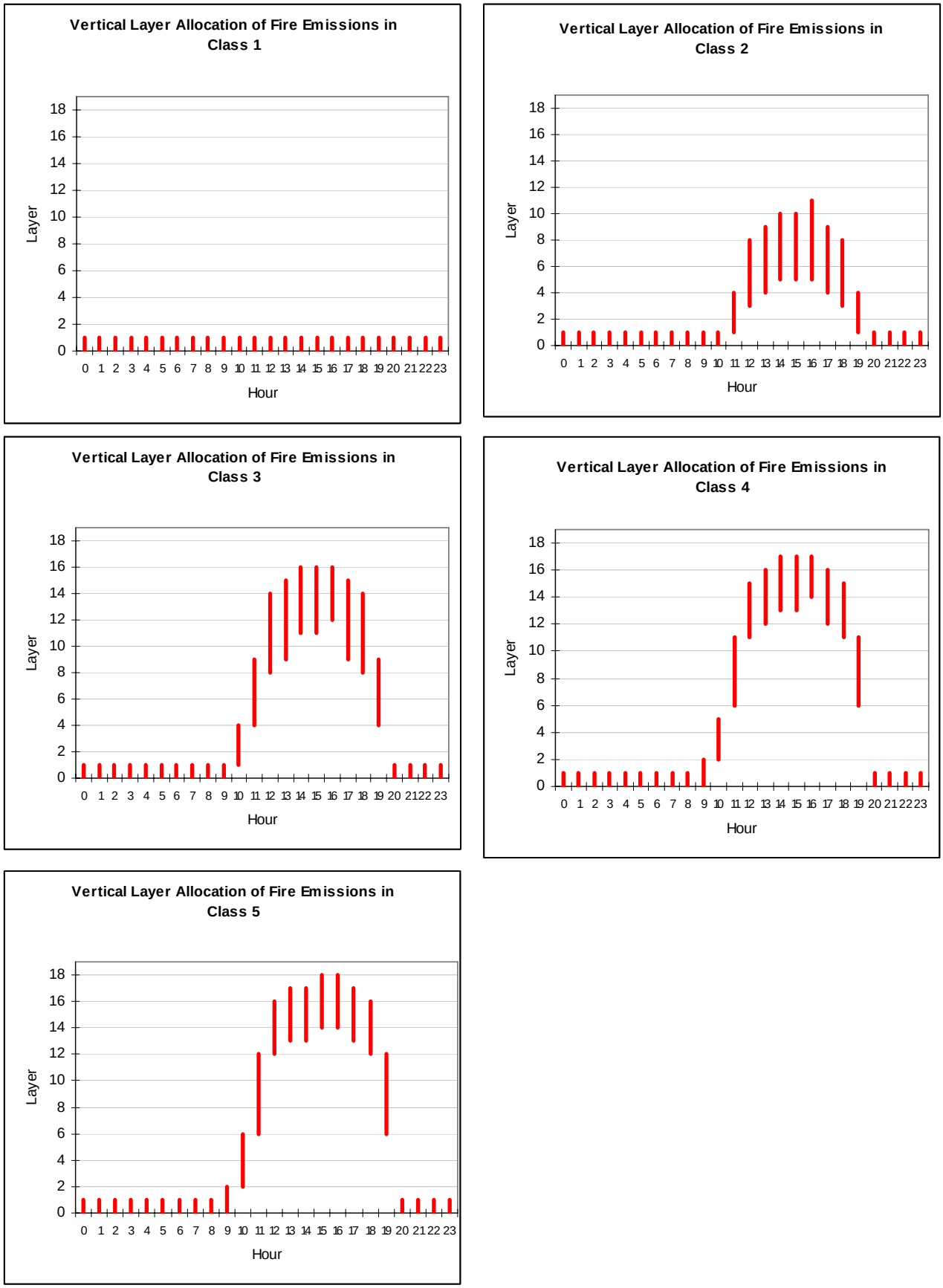

Figure 2-14. Vertical layer allocation of fire point sources by hour of the day for each fire class.

PSTFIR was also run using the 28-layer vertical structure for the TCEQ domain. The vertical layer interfaces were obtained from http://www.tceq.state.tx.us/implementation/air/airmod/data/hgb8h2/hgb8h2_camx_domain.html.

PIGEMS

The PIGEMS module combines elevated point source outputs from PSTFIR and PSTPNT and generates a CAMx-ready binary point source file. Since PSTFIR split each fire point into multiple points in vertical layers that differ from hour to hour, PIGEMS was modified to prevent fire points from being PiGged or regrouped as co-located points.

GRDEM

The GRDEM module allocates countywide area source emissions into gridded emissions. Grid surrogates for spatial allocation of agricultural and prescribed burning emissions for the TCEQ and RPO modeling domains were derived from several sources of geospatial data. Because these fire emission sources were estimated for some individual specific crops, crop-specific GIS data were used in developing gridding surrogates where available. For non-crop specific fires emissions, spatial surrogates were based on more general agricultural land. Fire emissions associated with prescribed burning and forest management activities were spatially allocated based on forest lands and rangeland and/or shrubland, as appropriate. Crop-specific GIS data layers for several Midwest states and the Lower Mississippi Valley region were obtained from the USDA National Agricultural Statistics Service (NASS) website (http://www.nass.usda.gov/research/Cropland/SARS1a.htm). These data were developed as part of the USDA NASS Cropland Data Layer (CDL) Program and represent agricultural, as well as non-agricultural, lands throughout the region based on data for calendar year 20007. The primary purpose of the CDL Program is to use satellite imagery to (1) provide acreage estimates to the Agricultural Statistics Board for the state's major commodities and (2) produce digital, crop-specific, categorized geo-referenced output products.

The NASS CDL is a raster, geo-referenced, crop-specific land cover data layer with a ground resolution of 56 meters. The CDL is produced using satellite imagery from the Indian Remote Sensing RESOURCESAT-1 (IRS-P6) Advanced Wide Field Sensor (AWiFS) collected during the current growing season. Ancillary classification inputs include: the United States Geological Survey (USGS) National Elevation Dataset (NED), the USGS National Land Cover Dataset 2001 (NLCD 2001), and the National Aeronautics and Space Administration (NASA) Moderate Resolution Imaging Spectroradiometer (MODIS) 250 meter 16 day Normalized Difference Vegetation Index (NDVI) composites. Agricultural training and validation data are derived from the Farm Service Agency (FSA) Common Land Unit (CLU) Program. The NLCD 2001 is used as non-agricultural training and validation data. As noted on the NASS website, the strength and emphasis of the CDL is agricultural land cover. Figure 2-14 provides a display of the CDL data for the Midwest and Lower Mississippi Valley.

As the NASS data sets did not include all states within the US, particularly, several states within the TCEQ modeling domain, the National Land Cover Database for 2001 (NLCD 2001) were used to augment the CDL data for surrogate development. Note, however, that the NLCD 2001 includes only a general classification of agricultural lands (Pasture/Hay/Cultivated Cropland).

Table 2-10 presents the complete set of available land use classes in the combined CDL/NLCD GIS data used for in the development of spatial surrogate. Included in Table 2-10 are the specific LULC codes and descriptions, as well as more general landuse codes and descriptions assigned to the data. Table 2-11 summarizes the data sources used for each state within the TCEQ modeling domain(s).

A small portion of Northern Mexico is also within the TCEQ modeling domains for which fire emissions data were provided, primarily associated with managed burning of slash/logging debris. These emissions data were spatial allocated to the modeling domains based on the 2000 North America Land Cover data (http://eros.usgs.gov/products/satellite/mrlc2001.html) for forestlands.

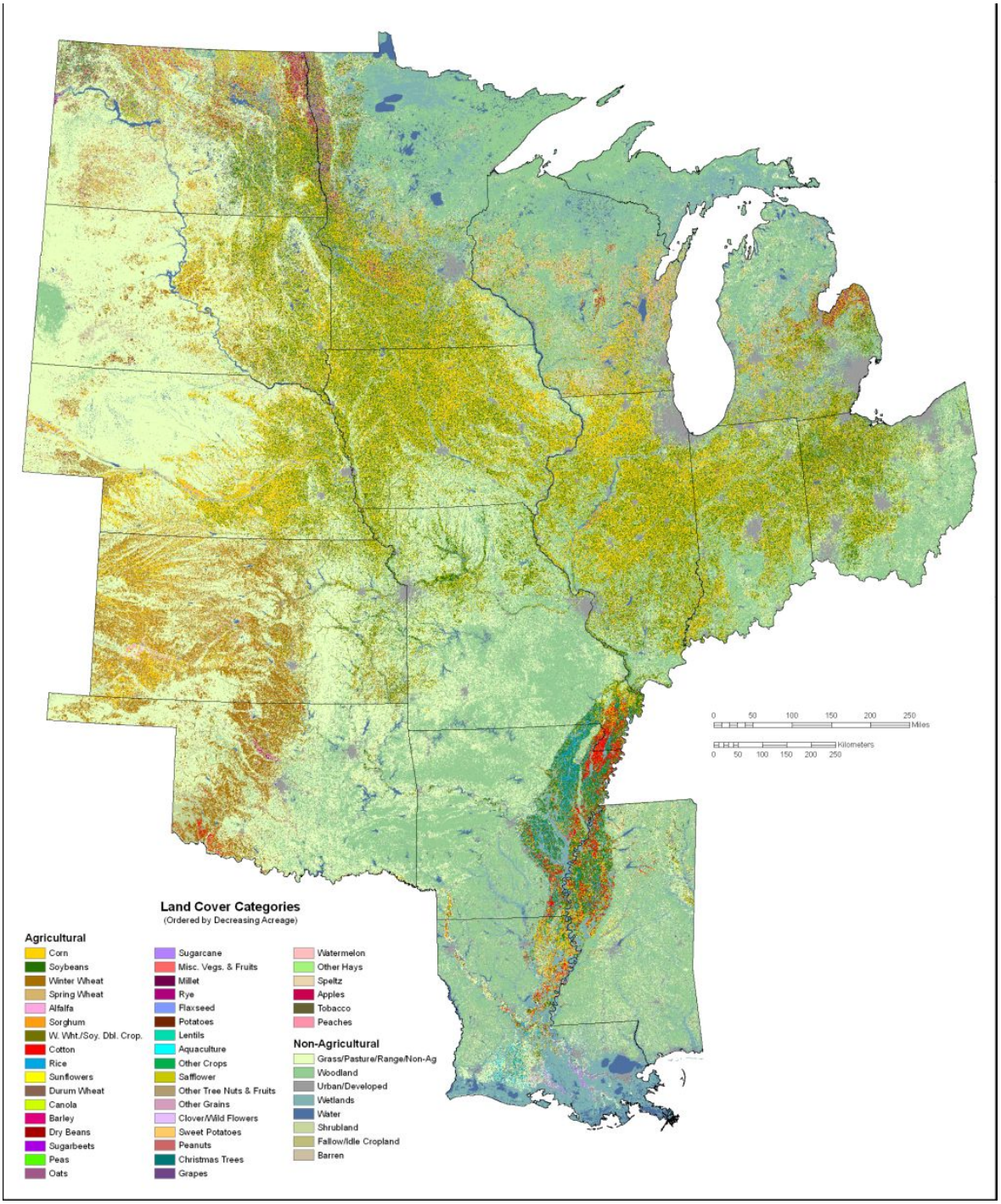

Figure 2-15. 2007 Cropland Data Layer for the Midwest and Lower Mississippi Valley. (Source: http://www.nass.usda.gov/research/Cropland/SARS1a.htm)

Table 2-10. Landuse/Landcover descriptions.

Grid-Code	LU-Code	Crop Description	LU Description
1	1000	Corn	Row Crops
2	1000	Cotton	Row Crops
3	1000	Rice	Row Crops
4	1000	Sorghum	Row Crops
5	1000	Soybeans	Row Crops
6	1000	Sunflowers	Row Crops
10	1000	Peanuts	Row Crops
11	1000	Tobacco	Row Crops
12	1000	Sweet Corn	Row Crops
13	1000	Popcorn or Ornamental Corn	Row Crops
21	2000	Barley	Grains/Hays/Seeds
22	2000	Durum Wheat	Grains/Hays/Seeds
23	2000	Spring Wheat	Grains/Hays/Seeds
24	2000	Winter Wheat	Grains/Hays/Seeds
25	2000	Other Small Grains	Grains/Hays/Seeds
26	2000	Winter Wheat/Soybeans Double-Cropped	Grains/Hays/Seeds
27	2000	Rye	Grains/Hays/Seeds
28	2000	Oats	Grains/Hays/Seeds
29	2000	Millet	Grains/Hays/Seeds
30	2000	Speltz	Grains/Hays/Seeds
31	2000	Canola	Grains/Hays/Seeds
32	2000	Flaxseed	Grains/Hays/Seeds
33	2000	Safflower	Grains/Hays/Seeds
34	2000	Rape seed	Grains/Hays/Seeds
35	2000	Mustard	Grains/Hays/Seeds
36	2000	Alfalfa	Grains/Hays/Seeds
37	2000	Other Hays	Grains/Hays/Seeds
38	2000	Camelina	Grains/Hays/Seeds
41	3000	Sugarbeets	Other Crops
42	3000	Dry Beans	Other Crops
43	3000	Potatoes	Other Crops
44	3000	Other Crops	Other Crops
45	3000	Sugarcane	Other Crops
46	3000	Sweet Potatoes	Other Crops
47	3000	Miscellaneous Vegetables & Fruit	Other Crops
48	3000	Watermelon	Other Crops
50	3000	Pickles	Other Crops
51	3000	Chick Peas	Other Crops
52	3000	Lentils	Other Crops
53	3000	Peas	Other Crops
56	3000	Hops	Other Crops
57	3000	Herbs	Other Crops
58	3000	Clover/Wildflowers	Other Crops
59	3000	Seed/Sod Grass	Other Crops
61	4000	Fallow/Idle Cropland	Open Non-Crop
62	4000	Grass/Pasture/Non-agricultural	Open Non-Crop
63	4000	Woodland	Open Non-Crop
64	4000	Shrubland	Open Non-Crop
65	4000	Barren	Open Non-Crop

Grid-Code	LU-Code	Crop Description	LU Description
67	5000	Peaches	Tree Crops
68	5000	Apples	Tree Crops
69	5000	Grapes	Tree Crops
70	5000	Christmas Trees	Tree Crops
71	5000	Other Tree Nuts & Fruit	Tree Crops
72	5000	Citrus	Tree Crops
73	5000	Other Tree Fruit	Tree Crops
80	5000	Other Non-Fruit Tree	Tree Crops
81	6000	Clouds	Other Non-Crops
82	6000	Urban/Developed	Other Non-Crops
83	6000	Water	Other Non-Crops
87	6000	Wetlands	Other Non-Crops
92	6000	Aquaculture	Other Non-Crops
111	7000	NLCD-Open Water	NLCD Non-Crop
112	7000	NLCD-Perennial Ice/Snow	NLCD Non-Crop
121	7000	NLCD-Developed/Open Space	NLCD Non-Crop
122	7000	NLCD-Developed/Low Intensity	NLCD Non-Crop
123	7000	NLCD-Developed/Medium Intensity	NLCD Non-Crop
124	7000	NLCD-Developed/High Intensity	NLCD Non-Crop
131	7000	NLCD-Barren	NLCD Non-Crop
141	7000	NLCD-Deciduous Forest	NLCD Non-Crop
142	7000	NLCD-Evergreen Forest	NLCD Non-Crop
143	7000	NLCD-Mixed Forest	NLCD Non-Crop
152	7000	NLCD-Shrubland	NLCD Non-Crop
171	7000	NLCD-Grassland Herbaceous	NLCD Non-Crop
181	7000	NLCD-Pasture/Hay	NLCD Non-Crop
182	7000	NLCD-Cultivated Crop	NLCD Non-Crop
190	7000	NLCD-Woody Wetlands	NLCD Non-Crop
195	7000	NLCD-Herbaceous Wetlands	NLCD Non-Crop

Table 2-11. Cropland data sources by state used for surrogate development in the TCEQ domain.

States Using CDL Data	States Using 2001 NLCD
Arkansas	Alabama
Iowa	Colorado
Illinois	Connecticut
Indiana	Delaware
Kansas	Florida
Louisiana	Georgia
Michigan	Kentucky
Minnesota	Massachusetts
Missouri	Maryland
Mississippi	Maine
Montana	North Carolina
North Dakota	New Hampshire
Nebraska	New Jersey
Ohio	New Mexico
Oklahoma	New York
South Dakota	Pennsylvania
Wisconsin	Rhode Island
	Tennessee
	Texas
	Virginia
	Vermont
	West Virginia
	Wyoming

Spatial allocation of county-level emission estimates is accomplished through the use of spatial surrogates or spatial allocation factors (SAFs) for each emission source category or group of source categories. Spatial surrogates are typically based on the proportion of a known region-wide characteristic variable, or variables, which exists within the region of interest. In the present case of agricultural and prescribed burning emissions the appropriate variables are agricultural lands, including crop-specific lands, forest and range/shrub lands. Spatial surrogates define the percentage of county level emissions from a particular source category that is to be allocated to some spatial region, typically a modeling grid cell. These percentages are based on areas of a type of agricultural land, or combinations of agricultural lands. The processing and development of gridding surrogates was performed using the Arc/INFO Geographic Information System (GIS) and the GIS data sources described above. Table 2-12 presents the definition, based on the LULC classifications available in the GIS data layers. An example of the "All Crops" surrogate for the TCEQ 36-km modeling domain is displayed in Figure 2-16, in terms of gridded surrogate density (km^2 surrogate/km^2 grid cell). Figure 2-17 displays the corresponding surrogate density for the TCEQ 12-km modeling domain. A complete set of displays for all surrogates developed as part of the project are presented in Appendix A.

Table 2-12. Spatial surrogate definitions.

Surrogate Code	Description	LULC Codes
TLA	Total Land Area	1, 2, 3, 4, 5, 6, 10,11, 12, 13, 21, 22, 23, 24, 25, 26, 27, 28, 29, 30, 31, 32, 33, 34, 35, 36, 37, 38, 41, 42, 43, 44, 45, 46, 47, 48, 50, 51, 52, 53, 58, 59, 61, 62, 63, 64, 65, 67, 68, 69, 70, 71, 72, 73, 80, 131, 141, 142, 143, 152, 171, 181, 182, 190, 195
ALF	Alfalfa	36
BAR	Barley	21
BEA	Dry Beans	42
COR	Corn	1, 12
GRS	Grasses	62
HAY	Other Hays	37
OAT	Oats	28
PEA	Peas	53
RIC	Rice	3
SOR	Sorghum	4
SUG	Sugarcane	45
WHE	Wheat	22, 23, 24, 26
ROW	Row Crops	1, 2, 3, 4, 5, 6, 10, 11, 12, 13,
GHS	Grains/Hays/Seeds	21, 22, 23, 24, 25, 26, 27, 28, 29, 30, 31, 32, 33, 34, 35, 36, 37, 38, 181
OTH	Other Crops	41, 42, 43, 44, 45, 46, 47, 48, 50, 51, 52, 53, 58, 59, 182
TRE	Tree Crops	67, 68, 69, 70, 71, 72, 73, 80
NTR	All Crops excluding Tree Crops	1, 2, 3, 4, 5, 6, 10, 11, 12, 13, 21, 22, 23, 24, 25, 26, 27, 28, 29, 30, 31, 32, 33, 34, 35, 36, 37, 38, 41, 42, 43, 44, 45, 46, 47, 48, 50, 51, 52, 53, 58, 59,181, 182
ALL	All Crops including Tree Crops	1, 2, 3, 4, 5, 6, 10, 11, 12, 13, 21, 22, 23, 24, 25, 26, 27, 28, 29, 30, 31, 32, 33, 34, 35, 36, 37, 38, 41, 42, 43, 44, 45, 46, 47, 48, 50, 51, 52, 53, 58, 59, 67, 68, 69, 70, 71, 72, 73, 80, 181, 182
GSR	Grassland/Shrubland/Rangeland	62, 64, 152, 171
FOR	Forest Land	63, 141, 142, 143

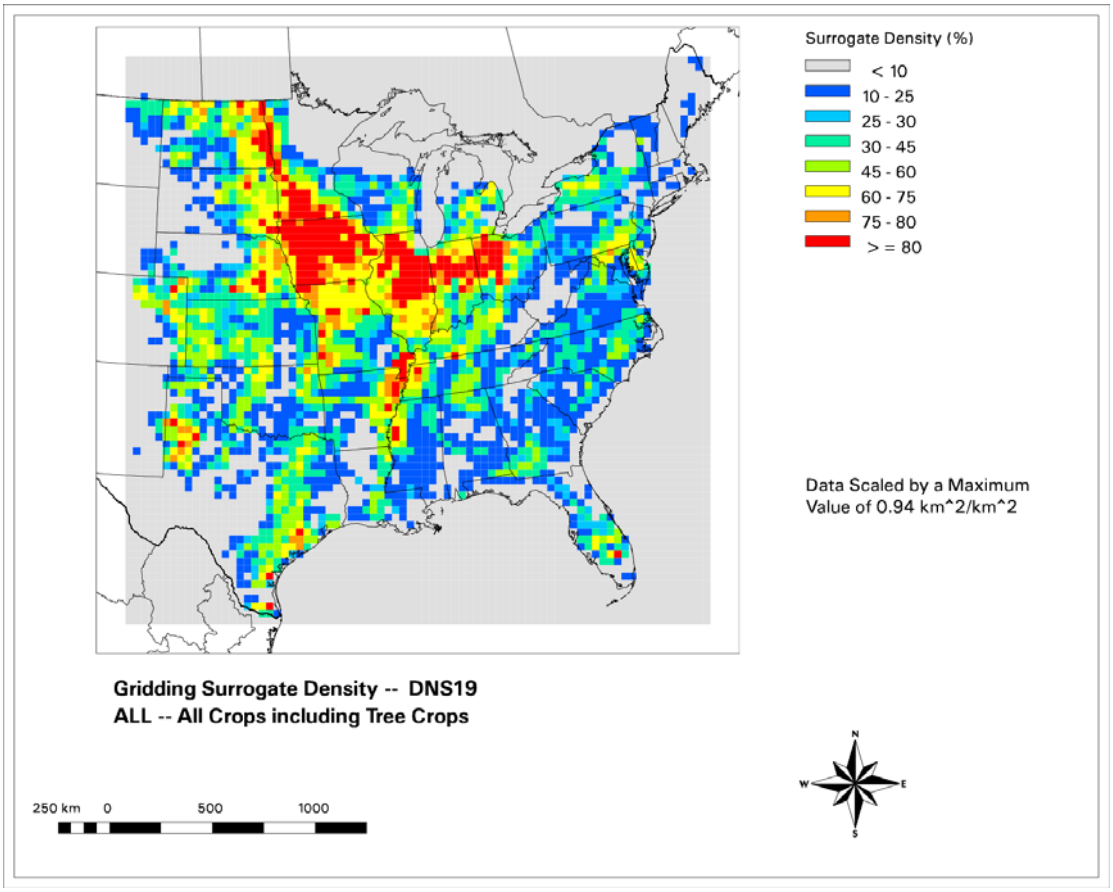

Figure 2-16. 36-km gridding surrogates for TCEQ Fire sources. Surrogate 19 – ALL – All Crops.

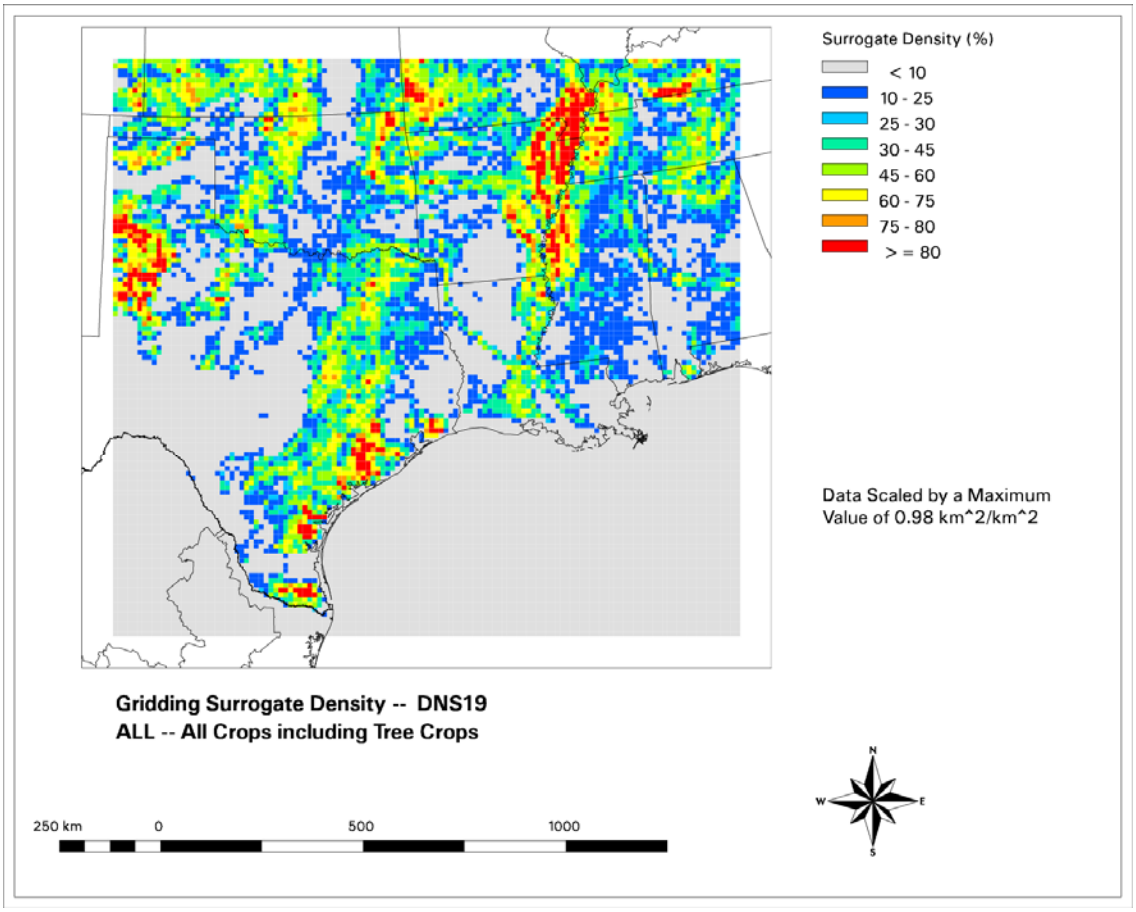

Figure 2-17. 12-km gridding surrogates for TCEQ Fire sources. Surrogate 19 – ALL – All Crops.

The Emissions Processing System, version 3 (EPS3) must be supplied with a cross-reference file which assigns a particular gridding surrogate to each Source Classification Code (SCC) in the emission inventory. Additionally, the latest version of EPS3 allows the (optional) use of secondary and tertiary surrogate assignments, by SCC, in order to prevent the loss of emissions during the spatial allocation processing of the emission inventory. This situation may arise due to inconsistencies between emission estimates and spatial data used in the allocation process, errors in the assignment of SCCs to emission sources, poor resolution/classification of LULC data or any combination of these issues. Table 2-13 presents the SCCs for agricultural and prescribed burning emissions within the inventory used for the project and the assigned spatial surrogate codes, as implemented in the EPS3 processing.

Table 2-13. Surrogate/SCC assignments for spatial allocation of fire emissions.

SCC	Source Category Description		Primary Surrogate	Secondary Surrogate	Tertiary Surrogate
2801500000	Agricultural Field Burning - whole field set on fire	Total, all crop types	ALL	ALL	TLA
2801500100	Agricultural Field Burning - whole field set on fire	Field Crops Unspecified	OTH	ALL	TLA
2801500111	Agricultural Field Burning - whole field set on fire	Field Crop is Alfalfa : Headfire Burning	ALF	GHS	ALL
2801500112	Agricultural Field Burning - whole field set on fire	Field Crop is Alfalfa: Backfire Burning	ALF	GHS	ALL
2801500130	Agricultural Field Burning - whole field set on fire	Field Crop is Barley: Burning Techniques Not Significant	BAR	GHS	ALL
2801500141	Agricultural Field Burning - whole field set on fire	Field Crop is Bean (red): Headfire Burning	BEA	OTH	ALL
2801500150	Agricultural Field Burning - whole field set on fire	Field Crop is Corn: Burning Techniques Not Important	COR	ROW	ALL
2801500170	Agricultural Field Burning - whole field set on fire	Field Crop is Grasses: Burning Techniques Not Important	GRS	GHS	ALL
2801500181	Agricultural Field Burning - whole field set on fire	Field Crop is Hay (wild): Headfire Burning	HAY	GHS	ALL
2801500182	Agricultural Field Burning - whole field set on fire	Field Crop is Hay (wild): Backfire Burning	HAY	GHS	ALL
2801500191	Agricultural Field Burning - whole field set on fire	Field Crop is Oats: Headfire Burning	OAT	GHS	ALL
2801500192	Agricultural Field Burning - whole field set on fire	Field Crop is Oats: Backfire Burning	OAT	GHS	ALL
2801500201	Agricultural Field Burning - whole field set on fire	Field Crop is Pea: Headfire Burning	PEA	OTH	ALL
2801500220	Agricultural Field Burning - whole field set on fire	Field Crop is Rice: Burning Techniques Not Significant	RIC	ROW	ALL
2801500240	Agricultural Field Burning - whole field set on fire	Field Crop is Sorghum: Burning Techniques Not Significant	SOR	ROW	ALL
2801500250	Agricultural Field Burning - whole field set on fire	Field Crop is Sugar Cane: Burning Techniques Not Significant	SUG	OTH	ALL
2801500261	Agricultural Field Burning - whole field set on fire	Field Crop is Wheat: Headfire Burning	WHE	GHS	ALL
2801500262	Agricultural Field Burning - whole field set on fire	Field Crop is Wheat: Backfire Burning	WHE	GHS	ALL
2810015000	Prescribed Burning for Forest Management	Total	FOR	GRS	TLA
2810001000	Forest Wildfires	Total	FOR	FOR	TLA
2810020000	Prescribed burning of rangeland		GSR	GSR	TLA
2610000500	Waste disposal, treatment, and recovery, open burning. Land clearing debris		FOR	FOR	TLA

3. CAMx MODELING

Fire emissions can significantly influence air quality near and downwind of the source. In order to address the fire emissions that could be transported into the TCEQ 36 km domain, CAMx runs were performed on the 19-layer RPO 36 km domain, which covers the entire continental US and large sections of Canada and Mexico, and includes the entire TCEQ domain when transposed to the RPO projection, as shown in Figure 3-1. Base-year (2005 and 2006) runs include the NCAR episodic fire emissions, which were processed through EPS3 and described in Section 2. Boundary conditions for the TCEQ domain could then be extracted from the CAMx outputs to account for fires outside the TCEQ domain, including fires from the western US, Mexico, Canada, Cuba, and the Bahamas.

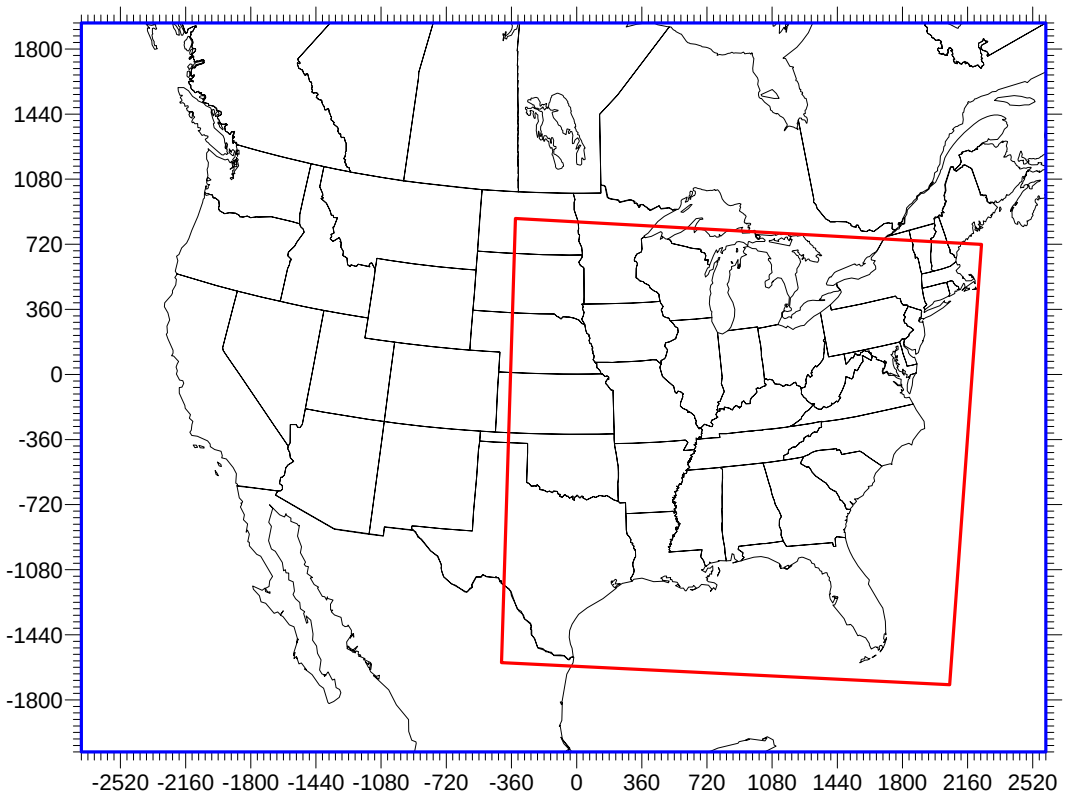

RPO 36 km (center 40N, 97W; true lats 33N, 45N)
148 x 112 (-2736, -2088) to 2592, 1944)

TCEQ 36km (center 40N, 100W; true lats 30N, 60N)
69 x 67 (-108, -1584) to (2376, 828)

Expressed in the RPO projection:
SW: (-414.84, -1593.96)
SE: (2060.40, -1715.88)
NE: (2236.80, 719.28)
NW: (-338.28, 862.74)

Figure 3-1. Map of the 36 km RPO and TCEQ domains.

Two periods were modeled using the RPO domain – May 1 to August 31, 2005, and May 1 to October 16, 2006 – and cover the five TCEQ episodes listed below with at least 18 days of model spin-up for each episode:

- May 19 – June 3, 2005
- June 17 – 30, 2005
- July 26 – August 8, 2005
- May 31 – June 16, 2006
- August 1 – October 15, 2006

3.1. CAMx INPUTS

Emissions

The 2005 and 2006 emissions were estimated by time-interpolating existing WRAP 2002b and 2018 inventories for all emission components except biogenics and fire emissions. These emissions were speciated to CB-IV.

Date specific biogenics for 2005 and 2006 were developed using MEGAN version 2.1 and were speciated to CB05. Episodic NCAR fire emissions were processed through EPS3. Both were added to the time-interpolated WRAP emissions, which were adjusted for the day of week, to complete the inventory. All emissions were in UTC.

Low-level emissions were merged together using MRGUAM. Elevated fire point sources were processed for each date using EPS3 and formatted for CAMx using PIGEMS. PIGEMS could not be used to merge the fire emissions with the WRAP point sources because the WRAP inventory was already in a CAMx binary format. Instead, a PTSMERGE program was used to merge the binary RPO point sources with the binary fire point source emissions.

Meteorology

The 2005 and 2006 CAMx meteorology fields were extracted from annual 36 km MM5 runs using MM5CAMx. The vertical diffusivity was based on the O'Brien profile with a minimum of 0.1 m^2/s. Extractions were made in UTC.

Boundary Conditions

For each period, two CAMx runs were performed using boundary conditions extracted from two global models -- the Model for Ozone And Related chemical Tracers (MOZART; Horowitz et al., 2003) and the Goddard Earth Observing Systems Chemistry (GEOS-Chem; Bey et al., 2001).

MOZART outputs were provided by Christine Wiedinmyer and Louisa Emmons at NCAR. The 2006 MOZART outputs were available in 6-hourly intervals for all species and dates in the episode. The 2005 MOZART outputs were only available from June to August. The 6-hourly outputs contained a limited number of species; corresponding 24-hourly outputs were used to

supplement some of the missing species. Table 3-1 lists the species available in 6 and 24-hourly intervals, and species not available for mapping to the CAMx CB05 species. The key species for ozone modeling, including O3 and NOx, were available in the 6-hourly files.

All dates in May, 2006 were averaged together to generate a monthly averaged, diurnally varying boundary condition file, which was used to represent the missing May dates in 2005.

The MOZART2CMAQ program read in MOZART outputs and was recently updated to map to the CAMx CB05 species, as listed in Table 3-2. The lowest 24 layers of MOZART were used to avoid the high levels of ozone in the stratosphere. Boundary conditions were extracted for the RPO domain in the CMAQ format. The CMAQ2UAM program converted from CMAQ to CAMx format; data was time-interpolated from the 6-hr or 24-hr averages to hourly outputs.

Boundary conditions in the top layers of the RPO domain continued to show high ozone levels (well over 100 ppb in layer 19 in certain boundaries and time periods), so the boundary conditions in layer 17 were copied to layers 18 and 19 to reduce the stratospheric ozone impact.

Table 3-1. List of MOZART species available in 2005.

6-hourly	24-hourly	Not available
C2H6	BIGALK	BIGALD
C3H8	BIGENE	C2H5OH
CO	C10H16	C2H5OOH
HNO3	C2H4	CH2O
NO2	C3H6	CH3CHO
NO	CH3COCH3	CH3COCHO
O3	CH3OH	CH3COOH
PAN	ISOP	CH3COOOH
	NH3	CH3OOH
	SO2	CRESOL
	TOLUENE	DMS
	SO4	GLYALD
	NH4NO3	H2O2
	NH4	HO2NO2
	SOA	ISOPNO3
	OC1	MACR
	OC2	MPAN
	CB1	MVK
	CB2	N2O5
	DUST1	NO3
	DUST2	ONIT
	DUST3	ONITR
	DUST4	SA1
		SA2
		SA3
		SA4

Table 3-2. Mapping of MOZART to CAMx CB05 species

CAMx	MOZART
NO	NO
NO2	NO2
O3	O3
H2O2	H2O2
NXOY	NO3 + 2 N2O5
HNO3	HNO3
PNA	HO2NO2
CO	CO
FORM	CH2O + 2 GLYOXAL
ALD2	CH3CHO
PAN	PAN
ALDX	GLYALD
PANX	MPAN
NTR	ONIT + ONITR + ISOPNO3
ETOH	C2H5OH
MEOH	CH3OH
MEPX	CH3OOH
ETHA	C2H6
ROOH	C2H5OOH + C3H7OOH + POOH + ROOH + MEKOOH + ALKOOH + ISOPOOH + MACROOH + TERPOOH + TOLOOH
AACD	CH3COOH
PACD	CH3COOOH
PAR	C3H6 + BIGENE + 5 BIGALK + 1.5 C3H8 + 3 CH3COCH3 + 4 MEK
ETH	C2H4
OLE	C3H6 + 0.5 BIGENE
IOLE	0.5 BIGENE
ISOP	ISOP
ISPD	MACR + MVK
TERP	C10H16
TOL	0.5 TOLUENE
XYL	0.5 TOLUENE
CRES	CRESOL
OPEN	BIGALD
MGLY	CH3COCHO
SO2	SO2 + DMS
NH3	NH3
TOLA	0.5 TOLUENE
XYLA	0.5 TOLUENE
ISP	ISOP
TRP	C10H16
PSO4	SO4
PNO3	NH4NO3
PNH4	NH4
SOA5	0.4 SOA
SOA6	0.4 SOA
POA	0.0545 (OC1 + OC2)
PEC	0.12 (CB1 + CB2)
FCRS	1.35 (DUST1 + DUST2 + DUST3)
CCRS	1.35 DUST4
NA	SA1 + SA2 + SA3 + SA4
PCL	SA1 + SA2 + SA3 + SA4

Boundary conditions for 2005 and 2006 from the second global model, GEOS-Chem could not be obtained in time for this study; instead, 2002 GEOS-Chem outputs were used. The 2002 GEOS-Chem outputs were available in 3-hourly intervals. The GEOS2CMAQ and CMAQ2UAM programs were used to map the GEOS-Chem species to CAMx CB05 species, extract boundaries to the RPO domain, and linearly time interpolate to 1-hourly outputs. Monthly averaged and diurnally varying boundary conditions were used to represent 2005 and 2006. Like MOZART, the layer 17 boundary conditions were mapped to layers 18 and 19 to reduce the stratospheric ozone impact. A list of species mappings from GEOS-Chem to CAMx is shown in Table 3-3; CAMx species are on the left and GEOS-Chem species are on the right.

Table 3-3. Mapping of GEOS-Chem to CAMx CB05 species.

CAMx	GEOS-CHEM
NO2	NOx
O3	Ox - NOx
CO	CO
NXOY	2 N2O5
HNO3	HNO3
PNA	HNO4
H2O2	H2O2
NTR	R4N2
FORM	CH2O
ALD2	0.5 ALD2
ALDX	RCHO
PAR	0.333 PRPE + ALK4 +0.5 C3H8 + ACET + MEK + RCHO
OLE	0.333 PRPE
ETHA	0.5 C2H6
MEPX	MP
PAN	PAN
PANX	PPN + PMN
ISOP	0.2 ISOP
ISPD	MACR + MVK
TERP	ALPH + LIMO + ALCO
SO2	SO2 + DMS
NH3	NH3
CG5	0.5 SOG1 + 0.5 SOG2
CG6	0.5 SOG1 + 0.5 SOG2
CG7	SOG3
ISP	0.2 ISOP
TRP	ALPH + LIMO + ALCO
PSO4	SO4 + MSA
PNO3	NIT
PNH4	NH4
SOA5	0.417 SOA1 + 0.444 SOA2
SOA6	0.417 SOA1 + 0.444 SOA2
SOA7	1.050 SOA3
POA	0.0545 OCPI + 0.0545 OCPO
PEC	BCPI + BCPO
FCRS	DST1 + DST2
CCRS	DST3 + DST4
PCL	SALA + SALC
NA	SALA + SALC

Initial conditions were uniform in each layer. Ozone was set to 35 ppb in the first seven layers, and increased to 70 ppb in the top layer. Values for the top boundary concentrations are listed in Table 3-4, where O3 is also 70 ppb.

Table 3-4. Top boundary conditions (ppm for gases, ug/m^3 for aerosols).

NO	0.0000E+00
NO2	0.0000E+00
O3	0.7000E-01
PAN	0.0000E+00
NXOY	0.0000E+00
OLE	0.0000E+00
PAR	0.6533E-03
TOL	0.0000E+00
XYL	0.0000E+00
FORM	0.5005E-04
ALD2	0.1000E-04
ETH	0.0000E+00
CRES	0.1000E-08
MGLY	0.5000E-07
OPEN	0.5000E-07
PNA	0.2000E-08
CO	0.5000E-01
HONO	0.1000E-08
H2O2	0.2000E-03
HNO3	0.1000E-03
ISOP	0.0000E+00
SO2	0.1000E-04
SULF	0.1000E-29
NH3	0.1000E-04
PSO4	0.4008E-01
CPRM	0.1890E-04

Other Inputs

Albedo, haze, and ozone column data were processed using the AHOMAP software with daily Total Ozone Mapping Spectrometer (TOMS) data downloaded from http://toms.gsfc.nasa.gov/ozone/ozone_v8.html. Daily snow cover data were also added to take into account the high albedo of snow, which could be important in the mountain states. Snow cover data was extracted from MM5 for each date using MM5CAMx. Any grid cell that had snow cover at any hour during the day was considered covered in snow. Monthly ahomap outputs were generated.

A lookup table of photolysis rates for the CB05 chemical mechanism was generated from the tuv.4.0_1 program. Outputs were generated at 11 vertical layers up to 10 km for all combinations of albedo, haze, and ozone column bins defined in ahomap.

CAMx version 4.51 was run in UTC using the CB05 chemical mechanism in the RPO 36 km domain with 19 vertical layers. The 2005 and 2006 seasons were each run with boundary conditions extracted from GEOS-Chem and from MOZART. Three-dimensional outputs were generated so that boundary conditions could be extracted for the TCEQ 36 km domain.

3.2. CAMx RESULTS

Boundary Condition Extraction

Lateral boundary conditions for the TCEQ 36 km domain were extracted from CAMx outputs of the RPO domain, incorporating fire emissions from outside the TCEQ domain. The extraction consisted of three steps. First, the three-dimensional outputs were reprojected from the RPO projection to the TCEQ projection. Each layer was interpolated and windowed to the new projection; then, the 19 vertical layers from the RPO configuration were mapped to TCEQ's eastern US 17 layer structure. Next, boundaries were extracted using the existing bndextr program, and then they were time shifted from UTC to CST. Boundary conditions were extracted for all five TCEQ episodes in 2005 and 2006 from both the MOZART and GEOS-Chem runs.

Table 3-5 lists the reference state heights of the RPO vertical layer interfaces, assuming a sea level pressure and temperature of 1000 mb and 300K, respectively, and a temperature lapse rate of 50K when the pressure changes by a factor of e. Table 3-5 also lists the TCEQ 36 km domain's vertical layer interfaces, obtained from http://www.tceq.state.tx.us/implementation/air/airmod/data/hgb8h2/hgb8h2_camx_domain.html#layer, showing the RPO layer used to represent each of the 17 TCEQ vertical layers. All RPO layers were used except layers 3 and 12.

Table 3-5. Height interfaces of the RPO and TCEQ vertical layer structures.

Layer	RPO Height [m]	TCEQ 36 km Height[m]
19	16350	15179
18	8951	9167
17	5661	5836
16	3776	4106
15	2693	3026
14	1999	2103
13	1530	1353
12	1170	
11	995	1068
10	822	791
9	653	610
8	486	520
7	403	432
6	321	344
5	240	257
4	159	171
3	119	
2	79	85
1	40	34
0	0	0

Model Performance

Ozone model performance was evaluated at sites near the TCEQ 36 km boundaries to determine whether MOZART or GEOS-Chem yielded better boundary conditions for the TCEQ domain. Ozone data from EPA's Air Quality System (AQS) were formatted for the sites shown in Figure 3-2. All observations were time shifted to CST and were compared to CAMx outputs in the first layer, which were also time shifted to CST.

Evaluations were performed for sites along each boundary. The western boundary monitors (green) consisted of 39 sites located mostly in New Mexico, Colorado, and the Dakotas. The northern boundary sites (blue) contained 31 monitors, of which half were in Maine. The southern boundary sites (orange) had 10 monitors in southern Texas and Florida. Sites easily identified to be in urban cores, such as Miami, Denver, Albuquerque, and El Paso, were removed. The eastern border contained no sites since it was over the Atlantic.

Figures 3-3 to 3-5 display bar charts of daily normalized bias and error statistics for 1-hour ozone on the left and right, respectively, for each date in the three 2005 TCEQ episodes. The plots compare model performance between the CAMx runs using GEOS-Chem and MOZART boundary conditions, depicted in blue and yellow, respectively. Each figure evaluates performance for sites near the TCEQ western boundary (top), southern boundary (middle row), and northern boundary (bottom). Ideally, each date's normalized bias should be between ±15 %, and normalized error should be under 35 %, which are represented by the red lines. Observations less than 30 ppb were excluded from the statistics to avoid inflated biases and errors when normalizing by a small observed value.

In all three 2005 episodes, the normalized bias at the western boundary sites was negative on all dates. In the May 19-June 3 episode, the CAMx run using MOZART boundary conditions predicted more ozone than GEOS-Chem along all three boundaries. In the west, model performance was better when using MOZART since ozone was under predicted. In the north, performance was worse with MOZART as 1-hour ozone was over estimated, while GEOS-Chem's normalized bias and error met the performance goals on all dates.

In the June 17-30, 2005 episode, ozone did not appear as sensitive to the different boundary conditions as performance was mixed along all boundaries.

In the July 26 to August 8, 2005 episode, MOZART appeared to perform better than GEOS-Chem. On the western boundary, MOZART's normalized bias was less negative than GEOS-Chem on all dates; normalized error was also a little better on all dates. On the northern boundary, normalized bias was mixed, but normalized error was better with MOZART than GEOS-Chem on most dates. The southern sites also tended to favor MOZART, especially towards the end of the episode.

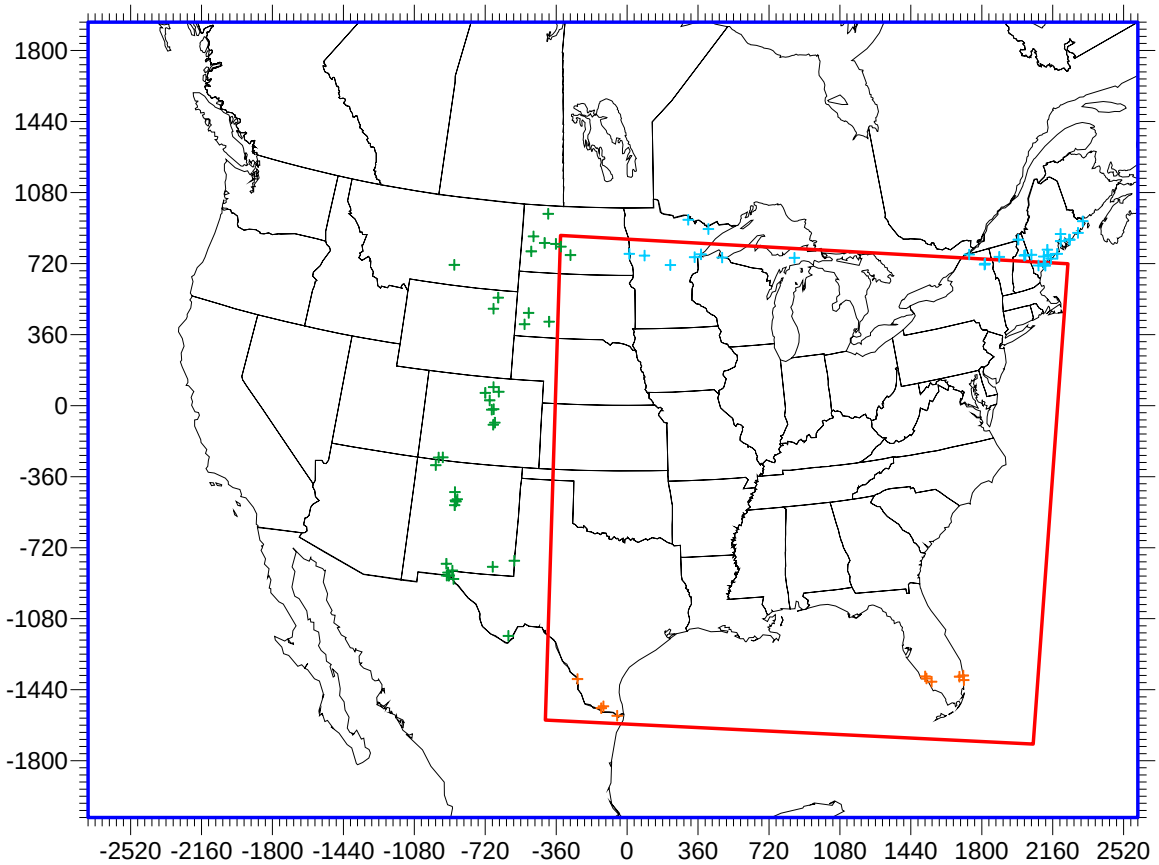

Figure 3-2. Map of AQS ozone monitoring sites near the TCEQ 36 km boundary.

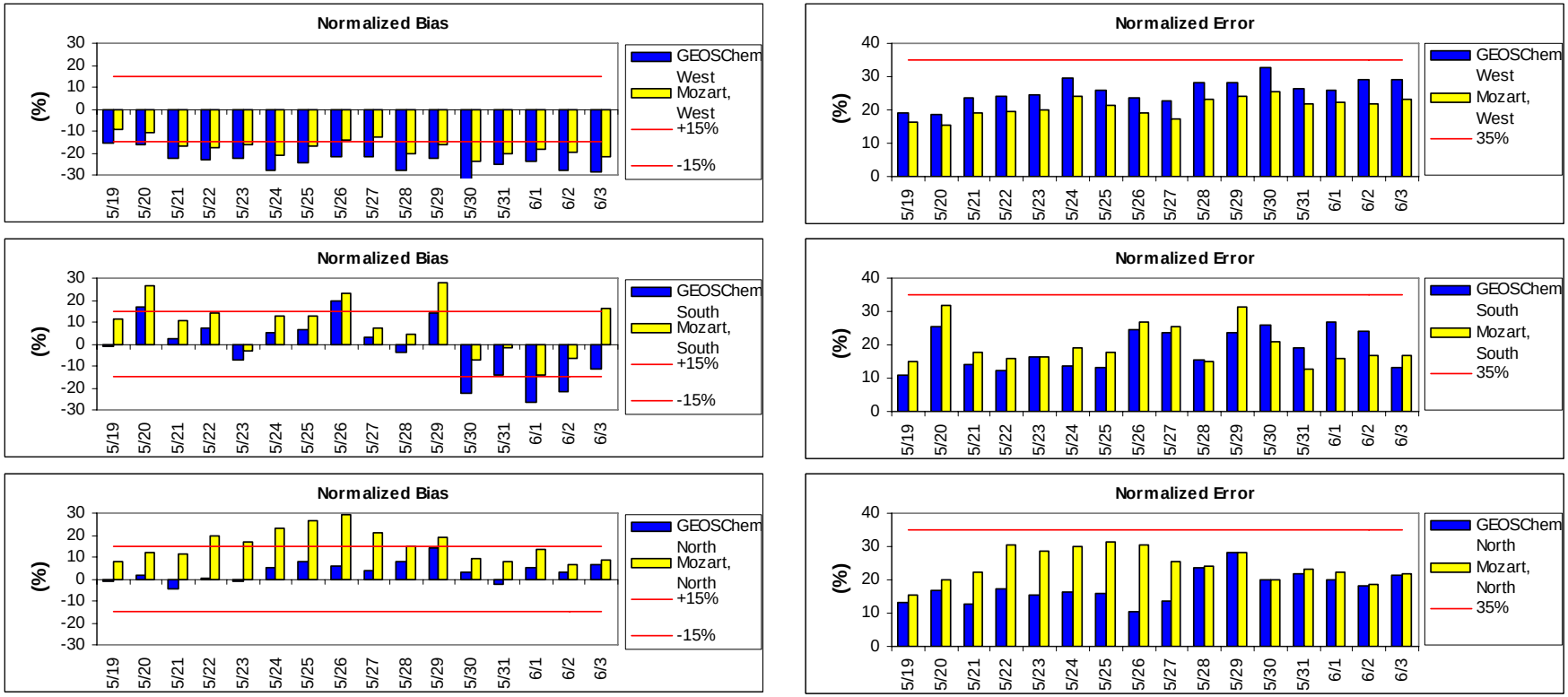

Figure 3-3. Normalized bias and error for 1-hour ozone at monitors near TCEQ's western, southern, and northern boundaries during the May 19-June 3, 2005 episode.

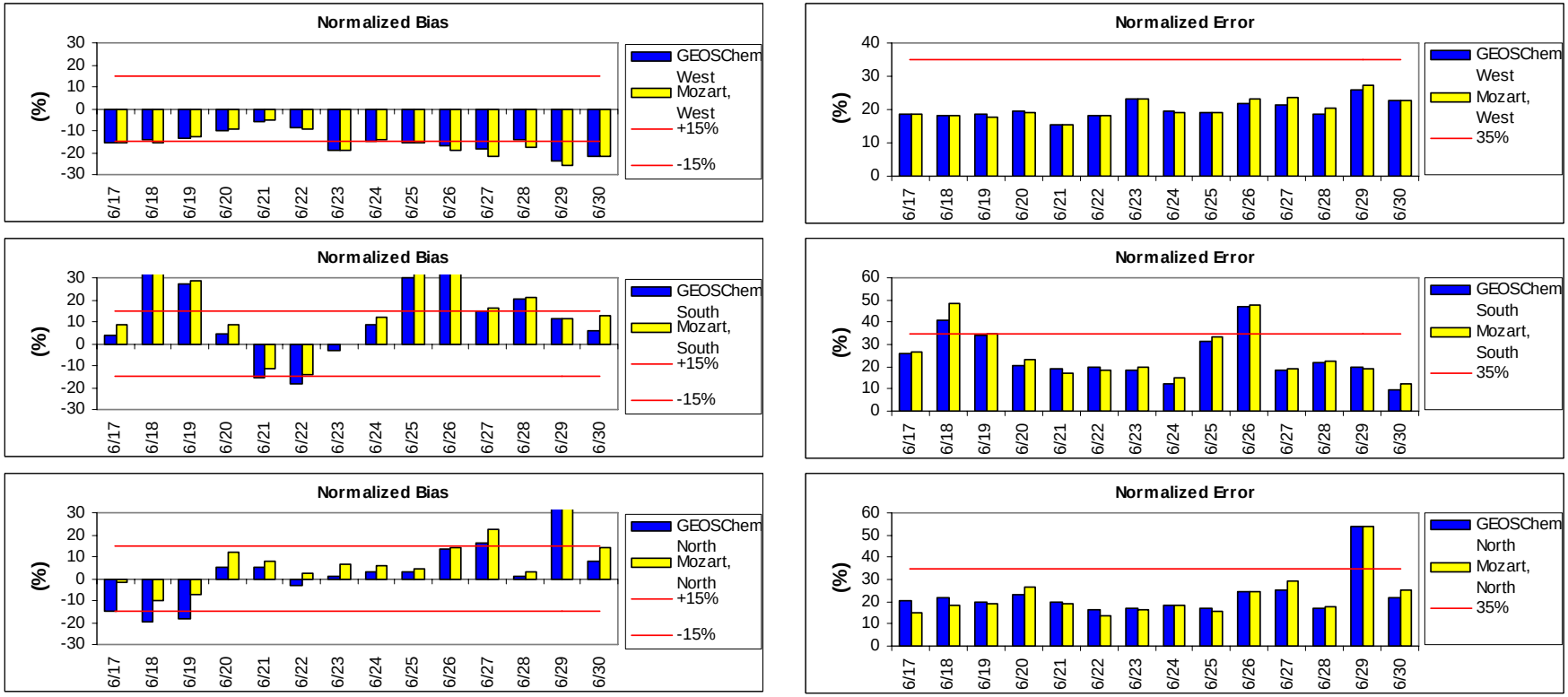

Figure 3-4. Normalized bias and error for 1-hour ozone at monitors near TCEQ's western, southern, and northern boundaries during the June 17 - 30, 2005 episode.

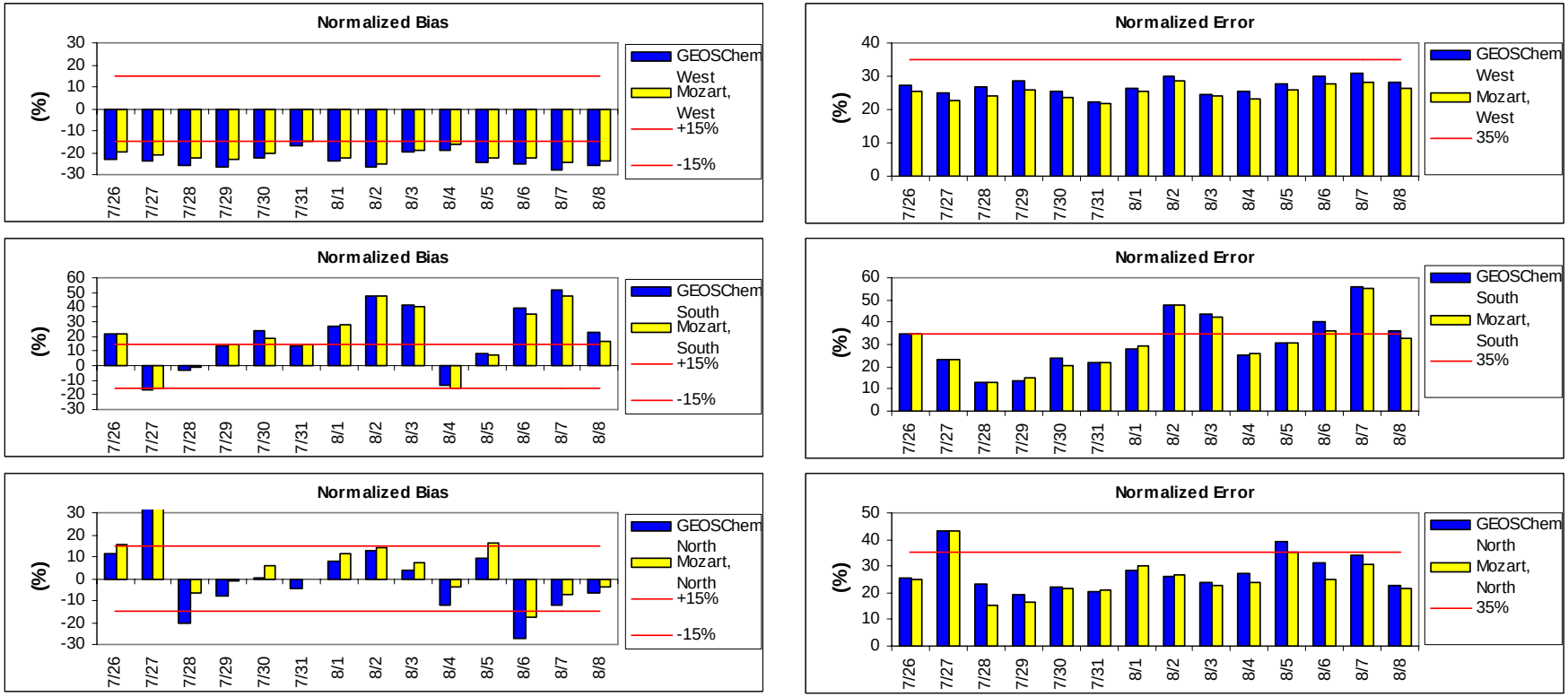

Figure 3-5. Normalized bias and error for 1-hour ozone at monitors near TCEQ's western, southern, and northern boundaries during the July 26 – August 8, 2005 episode.

Similar bar chart statistics are displayed in Figure 3-6 for the May 31 to June 16, 2006 episode. The western sites remained under predicted on all dates. The run with MOZART boundary conditions continued to perform better in the west compared to GEOS-Chem. GEOS-Chem performed better at the southern sites, particularly for normalized error on June 12. In the north, the normalized bias was positive on most dates when using MOZART boundary conditions, and negative when using GEOS-Chem. MOZART's normalized error was lower on most dates in the north.

Figure 3-7 shows similar plots for the August 1 to October 15, 2006 period. The plots were separated semi-monthly. MOZART boundary conditions performed better than GEOS-Chem at the western boundary sites throughout August and September as both runs under predicted 1-hour ozone, but MOZART contributed more. The use of MOZART boundary conditions met the normalized bias performance goals on many dates when GEOS-Chem did not. In October, GEOS-Chem performed better in the west as MOZART began to over predict ozone.

In the south, normalized bias was positive on all dates in August in both runs. Performance was worst on August 27, when both normalized bias and error exceeded 100 % in both runs. This was attributed to the low number of monitoring sites in the south and low ozone values measured at each site; there was only one observation greater than 30 ppb on this date among all southern boundary sites. In September and October, the GEOS-Chem run performed better than MOZART.

Near the northern boundary, MOZART's normalized bias was often positive while GEOS-Chem's was negative. Normalized error using MOZART boundary conditions appeared better on most dates in August, but became more mixed later in the period. On dates when the normalized error was highest (Aug 19, Sept 9 and 18, and Oct 4), MOZART's normalized error was usually worse than GEOS-Chem.

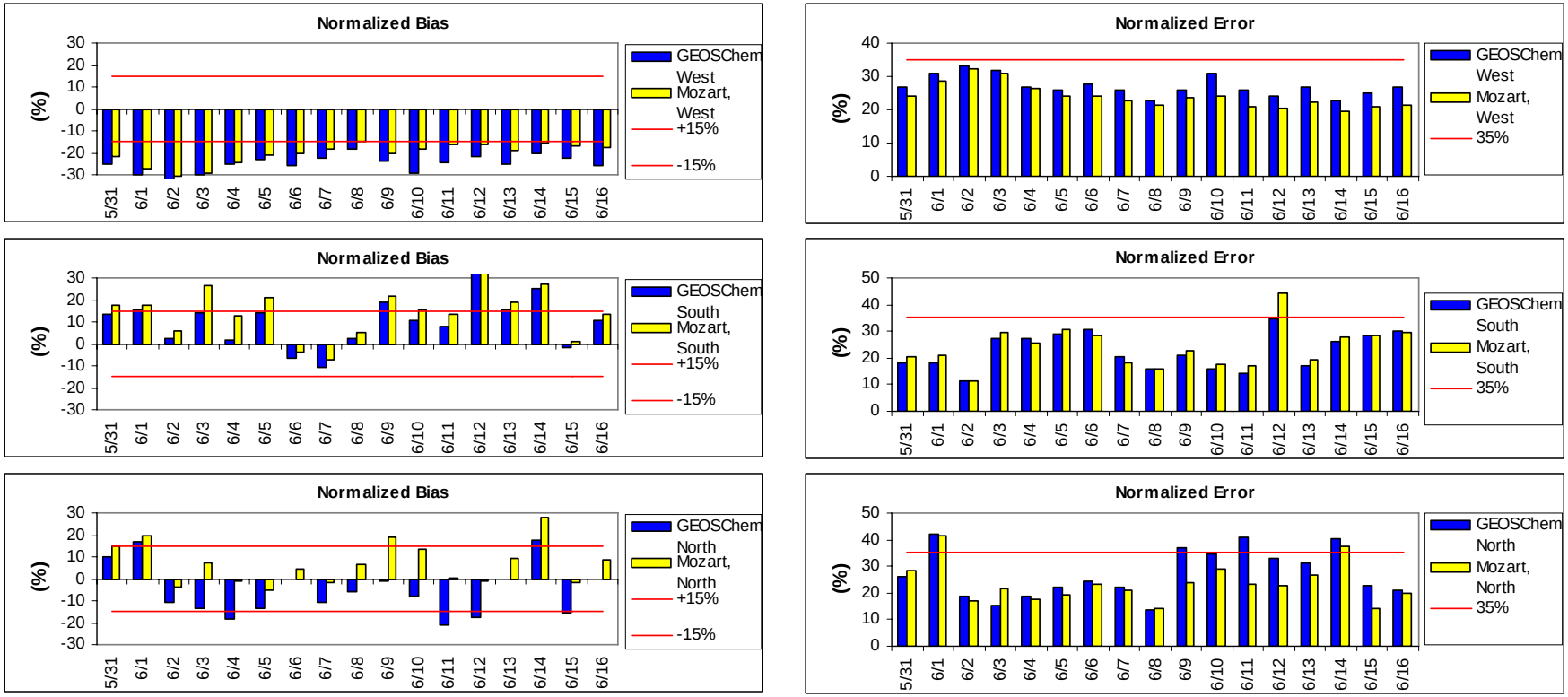

Figure 3-6. Normalized bias and error for 1-hour ozone at monitors near TCEQ's western, southern, and northern boundaries during the May 31 to June 16, 2006 episode.

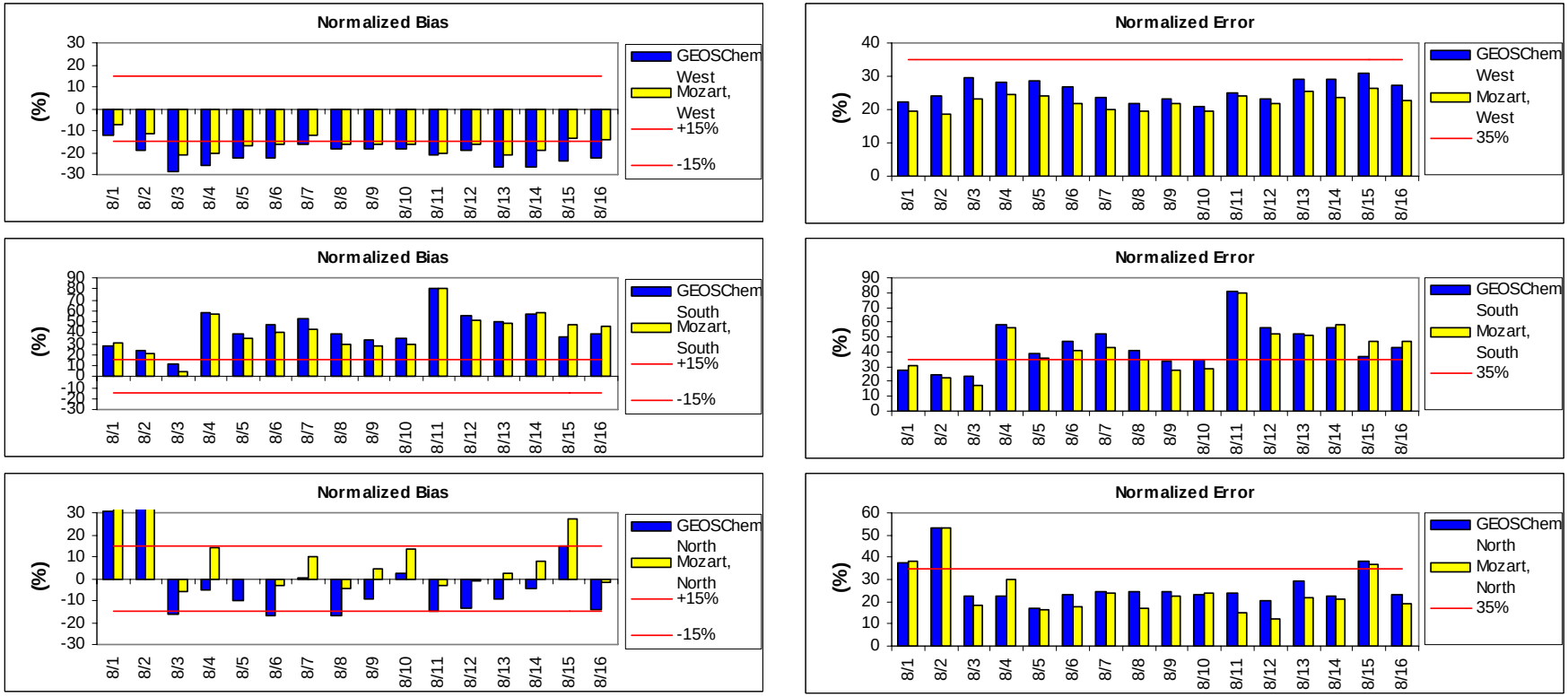

Figure 3-7 (continued). Normalized bias and error for 1-hour ozone at monitors near TCEQ's western, southern, and northern boundaries during the August 1 – October 15, 2006 episode.

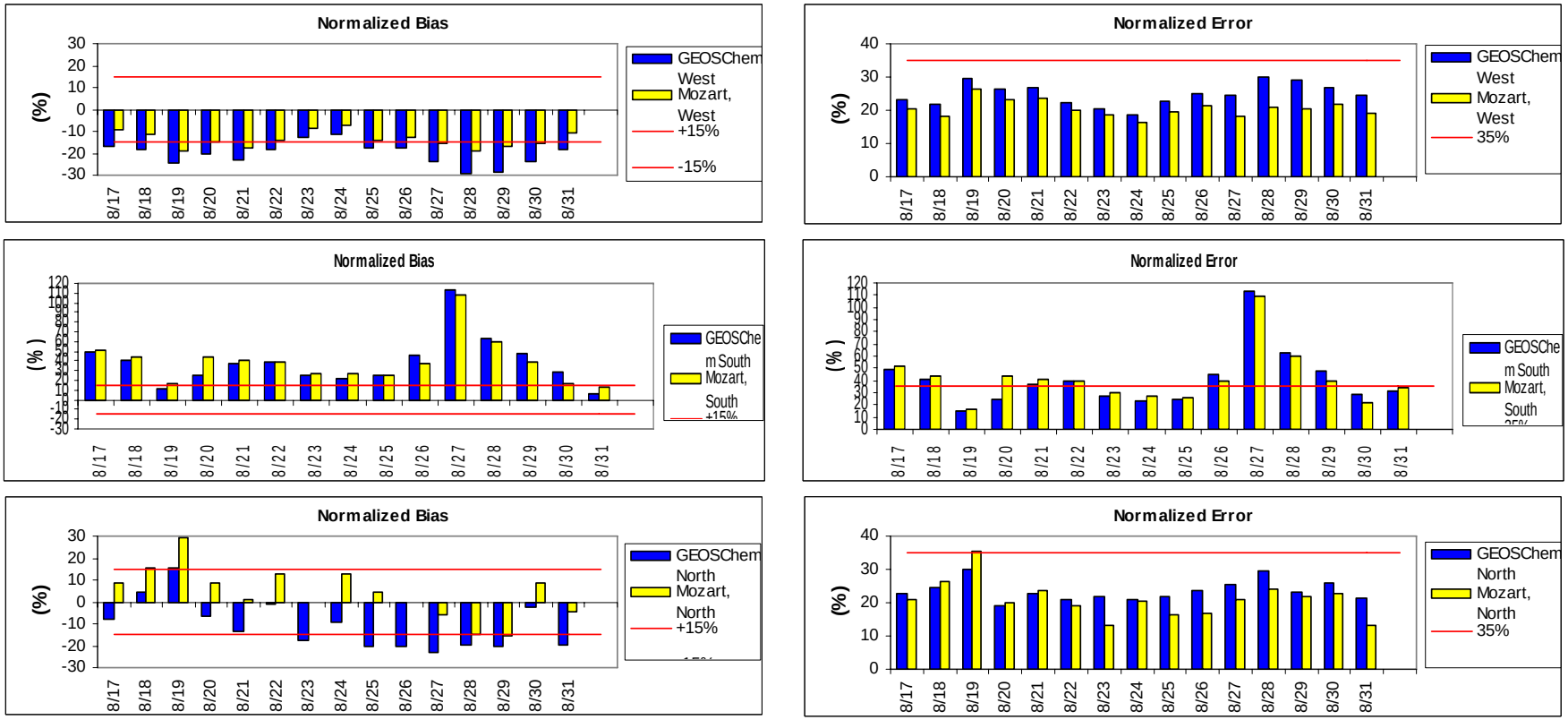

Figure 3-7 (continued). Normalized bias and error for 1-hour ozone at monitors near TCEQ's western, southern, and northern boundaries during the August 1 – October 15, 2006 episode.

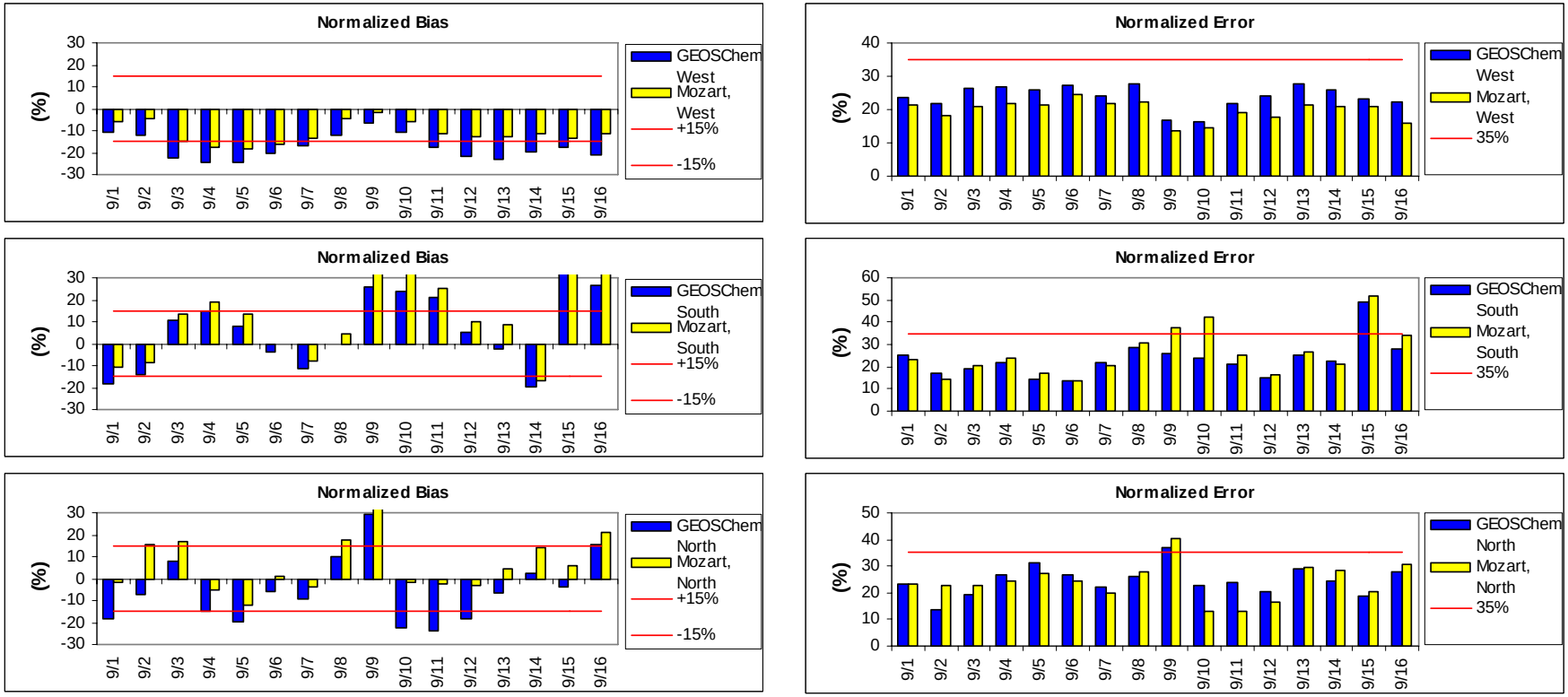

Figure 3-7 (continued). Normalized bias and error for 1-hour ozone at monitors near TCEQ's western, southern, and northern boundaries during the August 1 – October 15, 2006 episode.

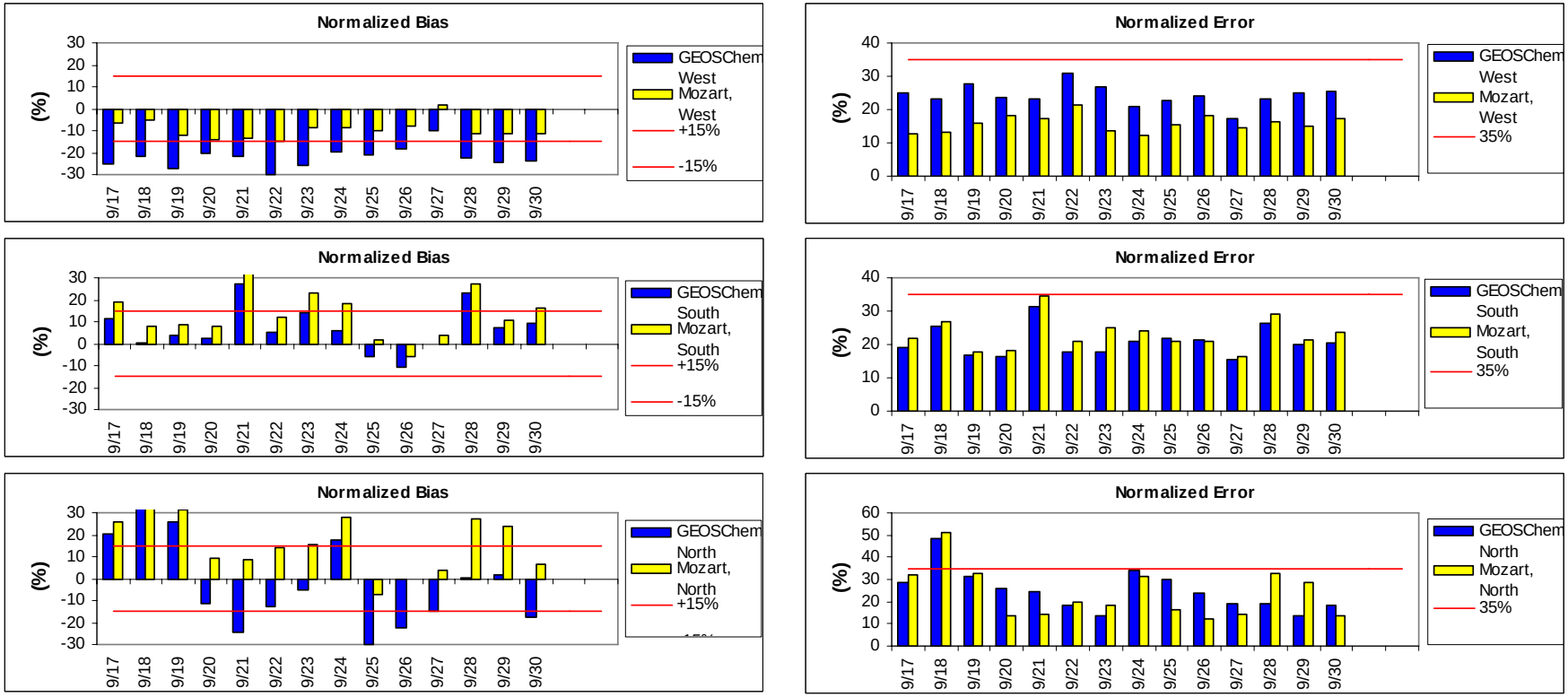

Figure 3-7 (continued). Normalized bias and error for 1-hour ozone at monitors near TCEQ's western, southern, and northern boundaries during the August 1 – October 15, 2006 episode.

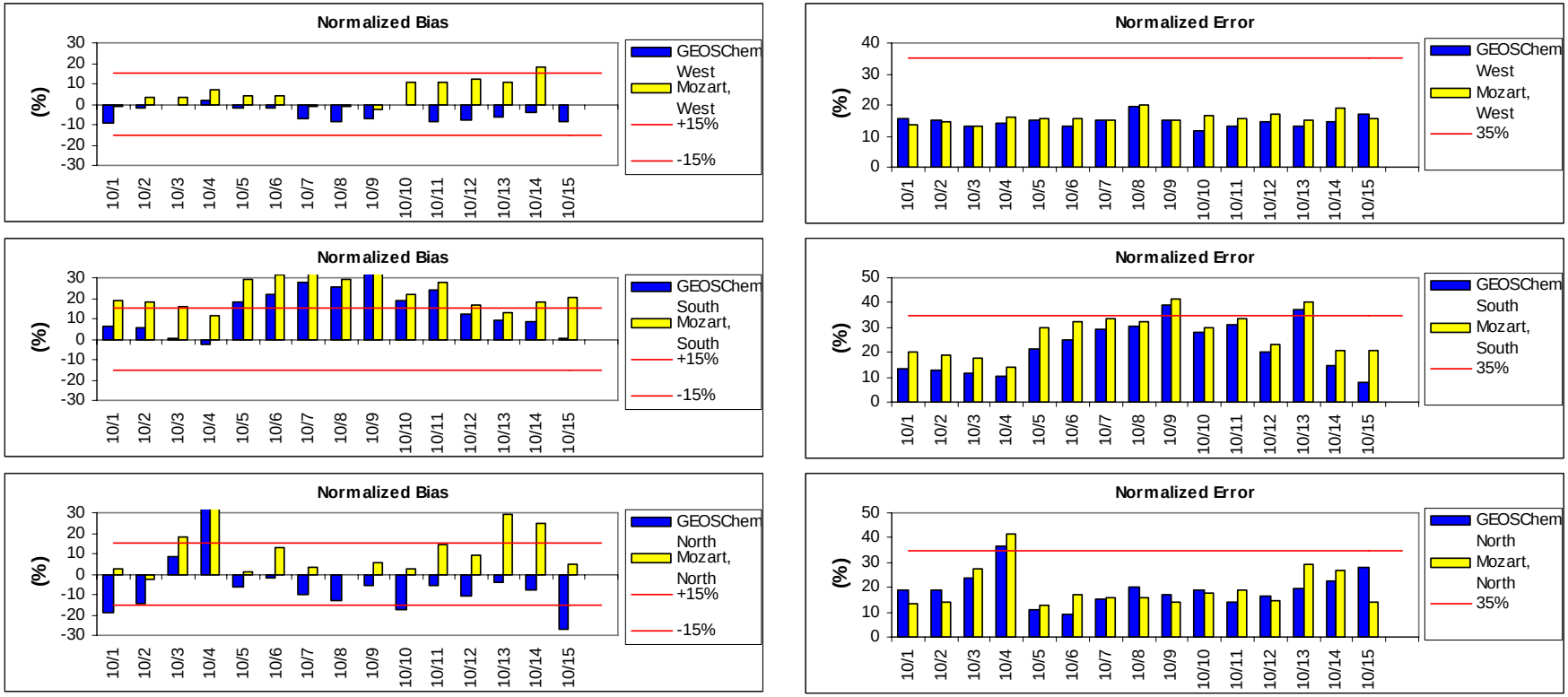

Figure 3-7 (concluded). Normalized bias and error for 1-hour ozone at monitors near TCEQ's western, southern, and northern boundaries during the August 1 – October 15, 2006 episode.

In the three 2005 episodes, the use of MOZART boundary conditions would greatly benefit model performance near TCEQ's western boundary, but could lead to over estimations near the northern boundary in the May 19 – June 3 episode. In 2006, model performance in the western sites was better when using MOZART while the southern sites were better using GEOS-Chem.

Several inert runs were performed to estimate the impact of ozone from the RPO 36 km boundaries. Impacts to Houston were examined. The two seasons were run with no emissions and no chemistry. One run examined ozone impacts from lateral and top boundary concentrations. A second run examined boundary condition impacts only by setting ozone in the top concentration file to 0. The difference between the two runs estimated the impact from the top boundary. Runs were performed using both the GEOS-Chem and MOZART boundary conditions.

Time series of 1-hourly ozone contributions to a grid cell over Houston from the top boundary, and from ozone in the MOZART and GEOS-Chem lateral boundaries are displayed in Figures 3-8 to 3-10 for each episode in 2005.

In the May 19 – June 3, 2005 episode, MOZART contributed more ozone to Houston than GEOS-Chem during all hours. The episode average 1-hour ozone contribution from MOZART and GEOS-Chem were 31 and 25 ppb, respectively, with greater contributions in the daytime. Peak 1-hourly contributions were 40 and 32 ppb from MOZART and GEOS-Chem, respectively. Ozone from the top boundary averaged 5 ppb.

In the June 17 – 30, 2005 episode, MOZART boundary contributions continued to contribute more ozone to Houston than GEOS-Chem, but the difference was much smaller than in the May, 2005 episode. This may help explain why model performance statistics shown in Figure 3-4 are relatively close.

In the July 26 – August 8, 2005 episode, MOZART contributions were the same or slightly higher than GEOS-Chem until the last three episode dates. The average lateral ozone contributions of 21 ppb and 22 ppb from GEOS-Chem and MOZART, respectively, were the lowest among the five episodes. Top boundary ozone contributions were very small in July, but increased in August.

Figures 3-11 and 3-12 display hourly boundary condition contributions to Houston in the two 2006 episodes. In the May 31 – June 16, 2006 episode, MOZART consistently contributed more than GEOS-Chem during the daytime peaks. In the August to October, 2006 period, lateral boundary contributions were comparable on most dates in August, except August 20, when MOZART's 1-hour ozone contribution spiked to 46 ppb – 12 ppb more than GEOS-Chem. This was the highest contribution in all of the five episodes. Contributions from both boundaries decreased in September as GEOS-Chem's and MOZART's monthly average contributions were only 16 and 21 ppb, respectively. Boundary contributions increased in October in both runs.

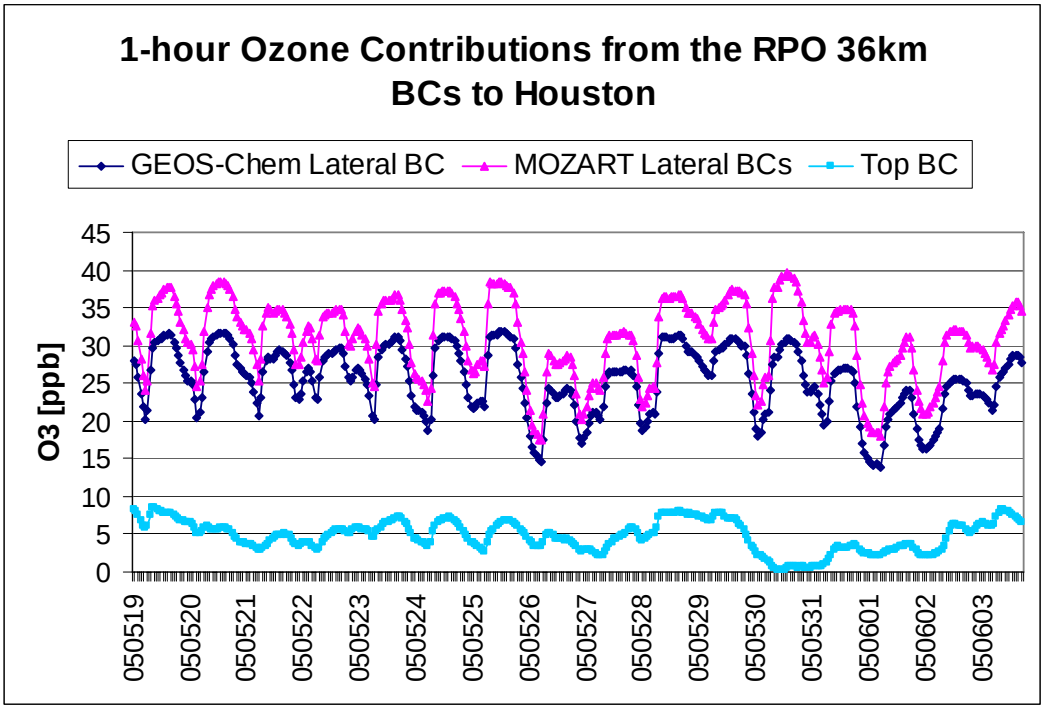

Figure 3-8. Ozone contributions from top and lateral boundaries from an inert run during the May 19 to June 3, 2005 episode.

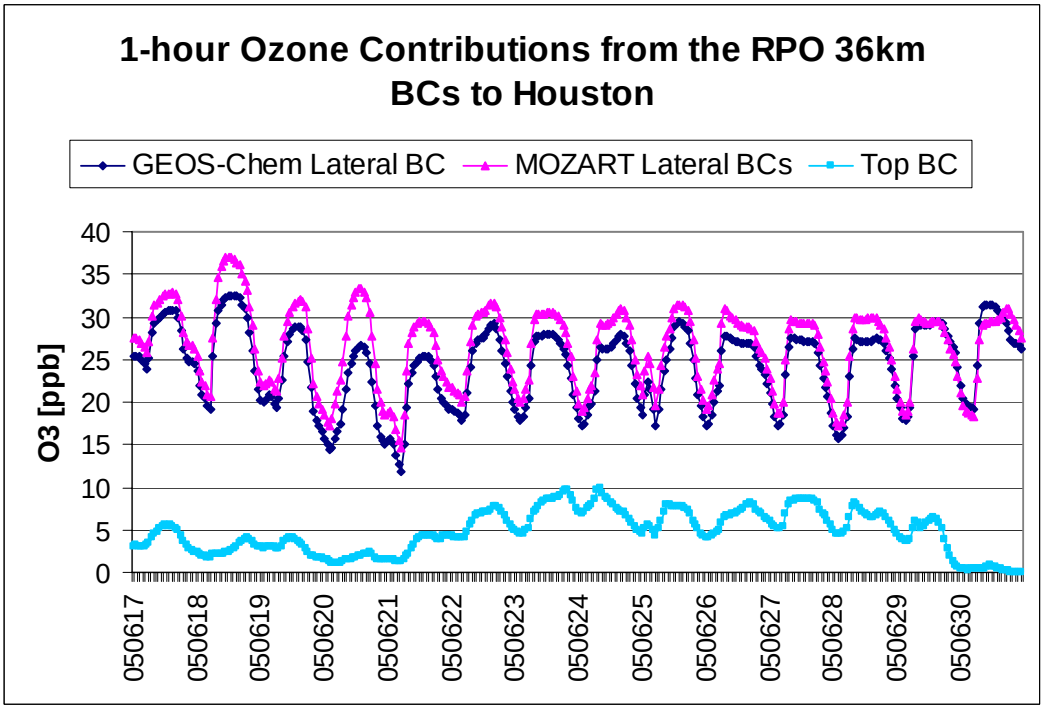

Figure 3-9. Ozone contributions from top and lateral boundaries from an inert run during the June 17-30, 2005 episode.

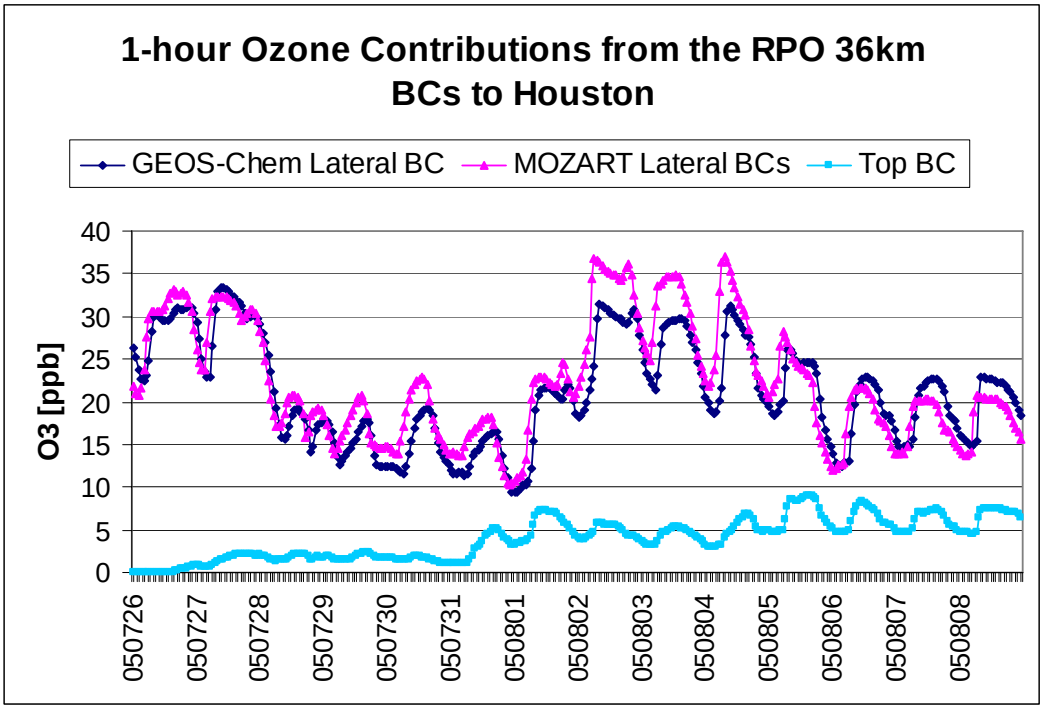

Figure 3-10. Ozone contributions from top and lateral boundaries from an inert run in the July 26 – August 8, 2005 episode.

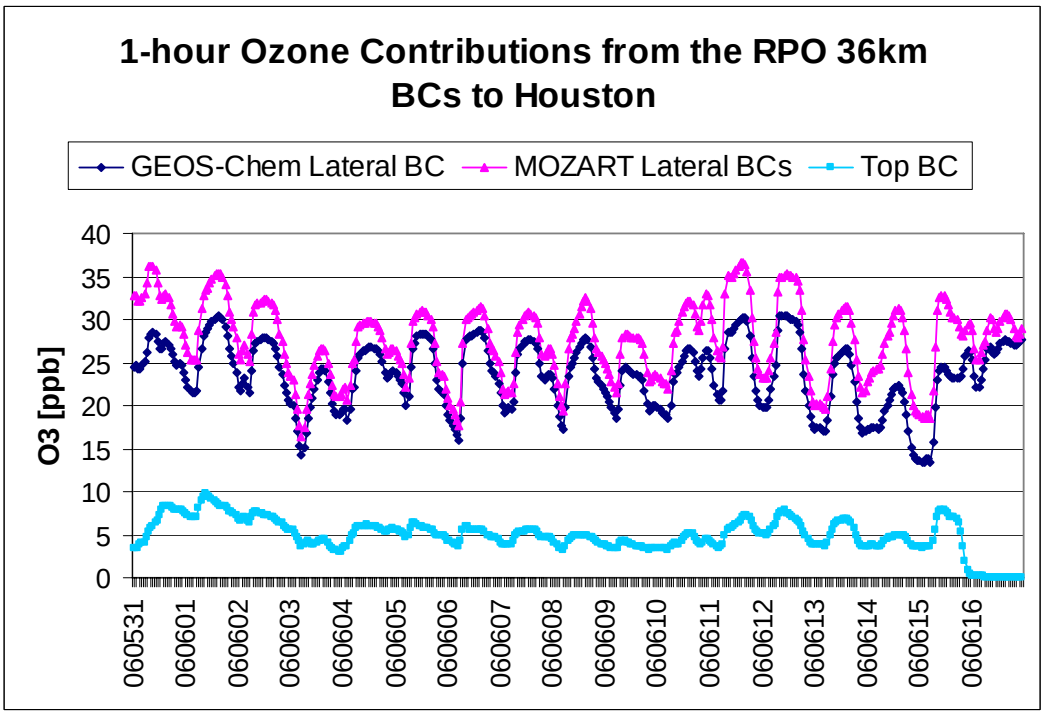

Figure 3-11. Ozone contributions from top and lateral boundaries from an inert run in the May 31 – June 16, 2006 episode.

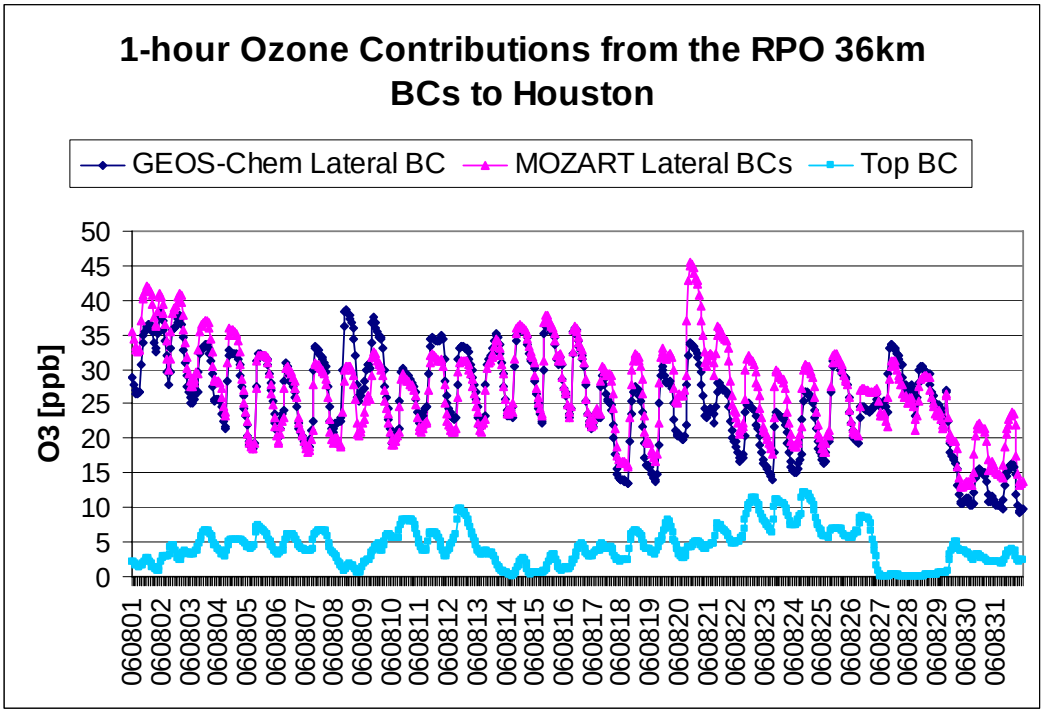

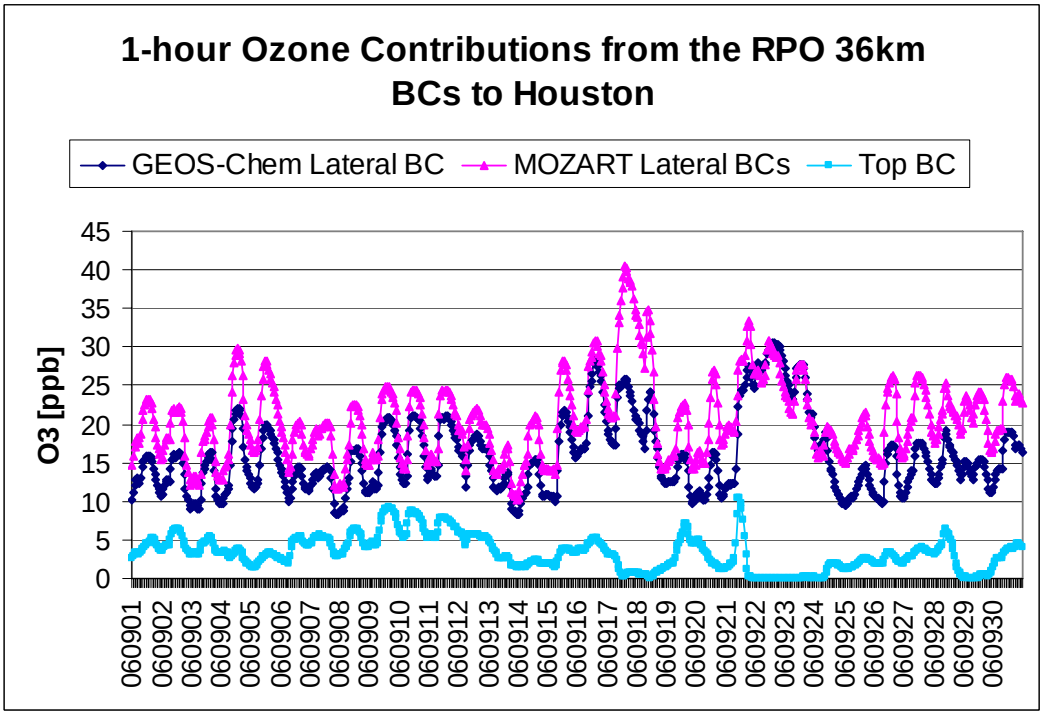

Figure 3-12. Ozone contributions from top and lateral boundaries from an inert run in the August 1 – October 15, 2006 episode.

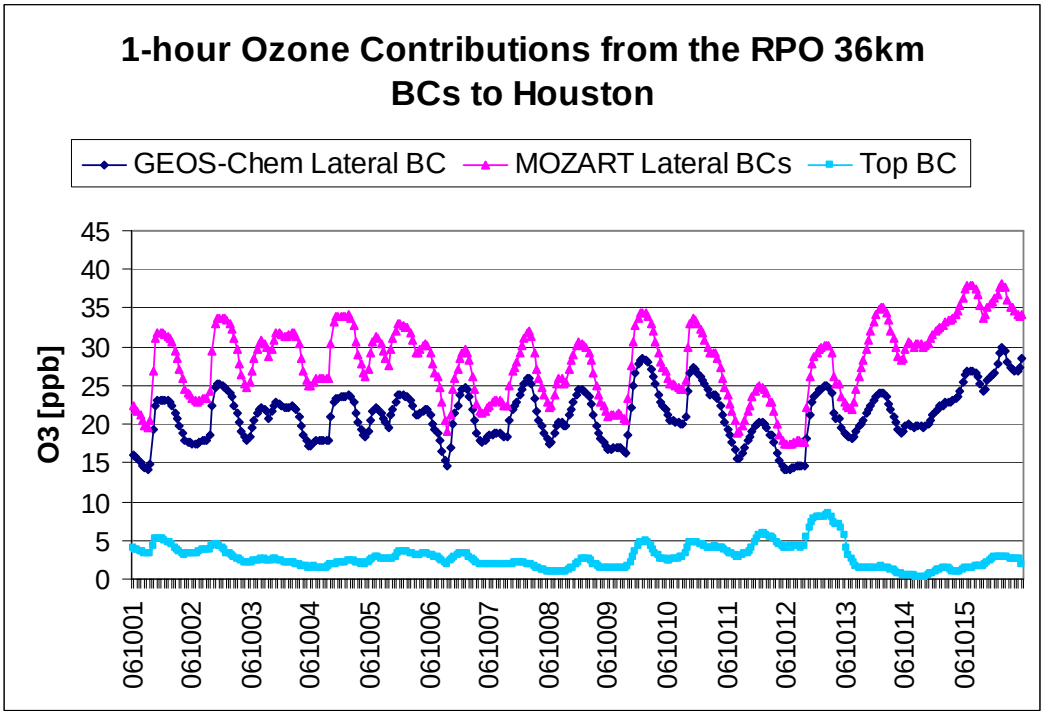

Figure 3-12 (concluded). Ozone contributions from top and lateral boundaries from an inert run in the August 1 – October 15, 2006 episode.

4. CAMx FUTURE YEAR MODELING

CAMx 2018 future year modeling of the May 1 to September 1, 2005 and May 1 to October 16, 2006 periods was performed for the 36 km RPO domain in order to extract future year boundary conditions for the TCEQ domain. Inputs were identical to the base year runs described in Section 3, except for the emissions.

In the 2005 and 2006 base years, CAMx generally produced better model performance for surface ozone near the boundaries of the TCEQ domain, particularly in the west, when using boundary conditions for the RPO domain derived from MOZART instead of GEOS-Chem, as discussed in Section 3. Assuming that better ozone performance at the surface is representative for the entire lateral boundaries, this section focuses on the CAMx simulations using MOZART boundary conditions. Future year simulations also were completed using GEOS-Chem boundary conditions, with boundary condition extractions of the TCEQ domain provided to TCEQ, but the results are not discussed here.

Future year emissions were based on the WRAP 2018 Preliminary Reasonable Progress (PRP18) inventory and typical fire emissions from the CENRAP Typical 02g inventory. As discussed in Section 3, the typical fire inventory consisted of point sources when the fire location and date were known; otherwise, the fire was treated as an area source. All emissions were adjusted to match the day of week of the base years.

4.1. TYPICAL FIRE EMISSIONS

Table 4-1 summarizes area source fire emissions from the CENRAP typical fire inventory for each weekday (Wednesday) from May to October, and for each region (RPOs, Canada and Mexico). WRAP states were excluded since all fires were treated as point sources. NOx, VOC, and CO fire emissions are listed for three fire types: agricultural burning, prescribed burning, and wildfires.

Agricultural burning from the CENRAP states emitted the most among the area source fires by type and region for each month evaluated. This does not necessarily mean that there is more agricultural burning in these states; it could be a result of a more complete inventory. In contrast, the fire emissions from the MRPO states had very little emissions from May to October. Illinois and Indiana were the only states in the MRPO domain that had fires in the inventory; the latter only included NH3 emissions. There were no agricultural burning emissions in any of the MRPO states.

Table 4-1. Typical area source fire emissions for a weekday from May to October.

	NOx [tpd]			VOC [tpd]			CO [tpd]		
	Ag burning	Pre-scribed	Wild	Ag burning	Pre-scribed	Wild	Ag burning	Pre-scribed	Wild
May									
CENRAP	60.4	2.6	42.3	130.4	25.4	92.9	1355.6	438.9	1972.7
MANE-VU	0.4	0.0	1.0	2.8	0.1	2.1	23.3	0.3	45.1
MRPO	0.0	0.0	0.0	0.0	0.0	0.0	0.0	0.0	0.0
VISTAS	2.9	11.4	10.1	33.8	22.7	40.1	247.9	481.8	391.8
Canada	0.0	0.5	26.9	0.0	2.2	109.7	0.0	14.1	900.3
Mexico	0.0	9.8	0.7	56.3	14.0	4.4	619.2	139.2	25.7
Total	63.7	24.2	81.1	223.3	64.3	249.3	2246.0	1074.3	3335.6
June									
CENRAP	69.8	7.2	5.5	144.6	66.1	12.1	1836.4	1134.2	255.6
MANE-VU	0.0	0.0	2.0	0.0	0.2	11.6	0.0	1.4	71.6
MRPO	0.0	0.0	0.0	0.0	0.0	0.0	0.0	0.0	0.0
VISTAS	2.2	9.7	4.1	24.1	20.1	16.3	179.2	427.5	160.5
Canada	0.0	0.5	38.3	0.0	2.2	156.3	0.0	14.1	1282.6
Mexico	0.0	0.0	7.2	0.0	0.0	43.2	0.0	0.0	252.2
Total	72.0	17.4	57.2	168.8	88.6	239.5	2015.6	1577.2	2022.5
July									
CENRAP	112.5	4.7	25.2	196.9	33.7	55.3	2845.5	545.8	1174.5
MANE-VU	0.0	0.0	0.4	0.0	0.1	0.9	0.0	0.3	17.4
MRPO	0.0	0.0	0.0	0.0	0.0	0.0	0.0	0.0	0.1
VISTAS	0.3	10.5	2.4	4.0	22.2	9.5	29.5	472.5	90.7
Canada	0.0	0.8	33.2	0.0	3.7	135.3	0.0	24.0	1109.9
Mexico	0.0	0.0	7.2	0.0	0.0	43.2	0.0	0.0	252.2
Total	112.8	16.1	68.4	200.9	59.8	244.3	2875.1	1042.7	2644.8
August									
CENRAP	78.6	6.5	4.4	137.7	49.1	10.4	1788.1	804.9	205.6
MANE-VU	0.0	0.0	2.7	0.0	0.1	14.9	0.0	0.6	97.3
MRPO	0.0	0.0	0.0	0.0	0.0	0.0	0.0	0.0	0.0
VISTAS	0.4	12.8	2.7	5.4	26.2	11.6	39.2	556.7	98.2
Canada	0.0	0.9	16.6	0.0	3.9	67.6	0.0	25.4	555.0
Mexico	0.0	0.0	7.2	0.0	0.0	43.2	0.0	0.0	252.2
Total	79.0	20.2	33.6	143.0	79.3	147.7	1827.3	1387.7	1208.3
September									
CENRAP	168.4	6.3	2.4	292.3	45.8	6.7	3840.2	744.0	106.5
MANE-VU	0.1	0.0	1.5	0.8	0.1	3.0	6.7	0.5	55.2
MRPO	0.0	0.0	0.1	0.0	0.0	0.1	0.0	0.0	3.2
VISTAS	0.4	11.6	2.7	5.1	22.9	10.6	37.1	485.4	104.3
Canada	0.0	0.8	31.0	0.0	3.7	126.3	0.0	24.0	1035.9
Mexico	0.0	2.8	5.7	16.2	4.0	34.4	178.1	40.0	200.9
Total	168.9	21.6	43.4	314.3	76.5	181.1	4062.1	1294.0	1506.0
October									
CENRAP	177.8	6.0	3.2	332.5	45.6	7.0	4062.7	749.8	147.0
MANE-VU	0.1	0.1	0.2	0.8	0.5	0.4	6.7	8.4	9.3
MRPO	0.0	0.0	0.0	0.0	0.0	0.0	0.0	0.8	0.1
VISTAS	0.7	26.4	0.1	7.2	39.2	0.5	55.2	829.5	4.7
Canada	0.0	0.1	32.4	0.0	0.7	132.3	0.0	4.2	1085.3
Mexico	0.0	2.8	5.7	16.2	4.0	34.4	178.1	40.0	200.9
Total	178.6	35.5	41.7	356.7	90.1	174.7	4302.7	1632.7	1447.2

A summary of point source NOx, VOC, and CO emissions from fires in the CENRAP typical fire inventory is listed in Table 4-2. Since point sources are date-specific, only one date representing a Wednesday for each of the five TCEQ episodes is listed. Like Table 4-1, fire emissions are classified into agricultural burning, prescribed fires, and wild fires. Point sources were reported for WRAP, CENRAP, and VISTAS states only.

The typical wildfire emissions in the WRAP states were an order of magnitude larger than any other fire component – point or area – by region and fire type on each of these dates. Among the five dates, the WRAP wildfires on Wednesday, August 21, 2002 (which were used to represent Wednesday, August 23, 2006) had the greatest emissions, emitting almost 9000 tpd NOx and 20,000 tpd VOC. The second highest fire emissions came from the CENRAP agricultural burning area sources, which emitted 79 and 138 tpd NOx and VOC, respectively.

Using the same five Wednesdays, the total NOx, VOC, and CO typical fire emissions from point and area sources and from the entire RPO domain were compared to the 2005 and 2006 NCAR satellite-derived fire emissions on the corresponding dates, as shown in Table 4-3. Since typical fires represent a multi-year average and the NCAR data is date specific, no correlation was found (or expected) between the two inventories; the purpose of this comparison is to see whether the general magnitudes of emissions are similar in these two inventories. On May 25, 2005 and June 7, 2006, the NCAR fire inventory emitted almost twice as much NOx as the typical fire inventory; on the other three dates, the typical fire inventories were at least 40 % higher.

Table 4-4 compares the magnitude of NOx emissions from fires to emissions from all sources in the RPO domain for the five Wednesdays in the base and future years. In the base years, fire emissions accounted for 2 to 9 % of the total NOx emissions in the RPO domain on these five dates. In 2018, the total non-fire NOx emissions were 30 to 35 % lower than their corresponding base case NOx emissions on these five dates. The typical fires accounted for 1 % (June 7, 2006) to 16 % (August 23, 2006) of the daily total NOx emissions in 2018.

Table 4-2. Typical point source fire emissions on five Wednesdays.

	NOx [tpd]			VOC [tpd]			CO [tpd]		
	Ag burning	Pre-scribed	Wild	Ag burning	Pre-scribed	Wild	Ag burning	Pre-scribed	Wild
Wed., May 22, 2002 → Wed., May 25, 2005									
CENRAP	0.0	17.4	0.0	0.0	176.2	0.0	0.0	3065.2	0.0
VISTAS	0.0	11.5	33.7	40.2	25.6	73.9	261.6	490.8	1569.9
WRAP	19.2	70.0	765.0	32.8	156.4	1678.1	352.5	2169.6	35691.4
Total	19.2	98.9	798.7	73.0	358.2	1752.0	614.1	5725.7	37261.4
Wed., June 19, 2002 → Wed., June 22, 2005									
CENRAP	0.0	3.3	0.0	0.0	28.3	0.0	0.0	489.3	0.0
VISTAS	0.0	42.0	10.0	5.0	92.8	22.0	34.1	1890.3	467.2
WRAP	21.2	24.5	2114.4	41.1	57.5	4638.1	467.0	685.6	98593.5
Total	21.2	69.8	2124.5	46.1	178.5	4660.1	501.2	3065.2	99060.7
Wed., July 31, 2002 → Wed., August 3, 2005									
CENRAP	0.0	3.4	0.0	0.0	28.3	0.0	0.0	489.8	0.0
VISTAS	0.0	79.3	27.7	4.7	175.7	60.7	38.8	3519.7	1289.8
WRAP	21.1	12.9	2226.3	49.4	27.2	4883.4	532.9	569.7	103332.0
Total	21.1	95.6	2253.9	54.1	231.3	4944.1	571.6	4579.3	104621.8
Wed., June 5, 2002 → Wed., June 7, 2006									
CENRAP	0.0	9.1	0.0	0.0	115.8	0.0	0.0	2020.3	0.0
VISTAS	0.0	56.3	11.4	68.5	124.8	25.1	448.2	2482.4	533.5
WRAP	19.4	47.8	300.3	49.0	105.3	658.7	523.6	1634.6	14000.0
Total	19.4	113.2	311.7	117.5	345.8	683.8	971.8	6137.3	14533.5

	NOx [tpd]			VOC [tpd]			CO [tpd]		
	Ag burning	Pre-scribed	Wild	Ag burning	Pre-scribed	Wild	Ag burning	Pre-scribed	Wild
Wed., August 21, 2002 → Wed., August 23, 2006									
CENRAP	0.0	5.8	0.0	0.0	48.9	0.0	0.0	846.5	0.0
VISTAS	0.0	51.9	13.2	3.8	115.3	29.0	28.2	2264.6	616.9
WRAP	15.4	0.5	8961.5	22.9	0.8	19671.1	241.1	12.7	417600.0
Total	15.4	58.2	8974.8	26.8	165.0	19700.1	269.3	3123.8	418216.9

Table 4-3. Typical vs. satellite-derived fire emissions.

	NOx [tpd]		VOC [tpd]		CO [tpd]	
	NCAR	Typical	NCAR	Typical	NCAR	Typical
25-May-05	2252	1086	6746	2720	98200	50257
22-Jun-05	1692	2362	3462	5382	54200	108242
3-Aug-05	1127	2503	2454	5600	35900	114196
7-Jun-06	1228	591	2759	1644	41100	27258
23-Aug-06	6497	9181	13300	20262	211000	426033

Table 4-4. Fire and total NOx emissions in the base and future years.

	Base Year NOx [tpd]			Future Year NOx [tpd]		
	Fires	Total	% of Total	Fires	Total	% of Total
25-May-05	2252	69218	3.3%	1086	44709	2.4%
22-Jun-05	1692	73213	2.3%	2362	49250	4.8%
3-Aug-05	1127	74655	1.5%	2503	50818	4.9%
7-Jun-06	1228	67433	1.8%	591	47007	1.3%
23-Aug-06	6497	73536	8.8%	9181	56304	16.3%

4.2. FUTURE YEAR RESULTS

An evaluation of the two CAMx 2018 future year runs using MOZART-derived boundary conditions was performed by examining surface ozone at the same monitoring sites near the western, northern, and southern borders of the TCEQ 36 km modeling domain as in the base year. These sites were shown in Figure 3-2.

The 2018 daily average ozone using all sites near each lateral boundary was compared to the base year values to examine the change between the base and future years. Figure 4-1 displays time series of the daily average ozone from the CAMx 2005 and corresponding 2018 runs, both using MOZART boundary conditions, for sites near TCEQ's western (top), southern (middle) , and northern boundaries (bottom). The 2005 observed daily averages are also displayed for reference. Figure 4-2 shows time series of the differences between 2005 and 2018 from all three lateral boundaries.

Near TCEQ's western boundary, the 39-site daily average surface ozone was less than 2 ppb lower in 2018 than in 2005 on almost all dates. The May 19 to June 3 episode averaged a 0.8 ppb reduction in 2018. The June 17 to 30 and July 26 to August 8 episodes averaged 1.5 and 1.7 ppb reductions, respectively, in the future year.

Near the southern boundary, which averaged only 10 sites, the 2018 daily averages fluctuated ±4 ppb from the base year. The average change from 2005 to 2018 was -0.1 ppb in the May 19 to June 3 and July 26 to August 8 episodes, and +0.2 ppb in the June 17 to 30 episode.

The largest differences occurred near the northern boundary, which could be biased by the fact that half the monitors were located in Maine and are influenced by outflow from North America. The 2018 daily averages were lower than 2005 on most dates. The largest difference occurred on June 25, when 2018 was 12.4 ppb lower than the base year. The northern boundary in the May, June, and July/August, 2005 episodes averaged 2.6, 6.0, and 5.7 ppb lower, respectively, in 2018 than in 2005.

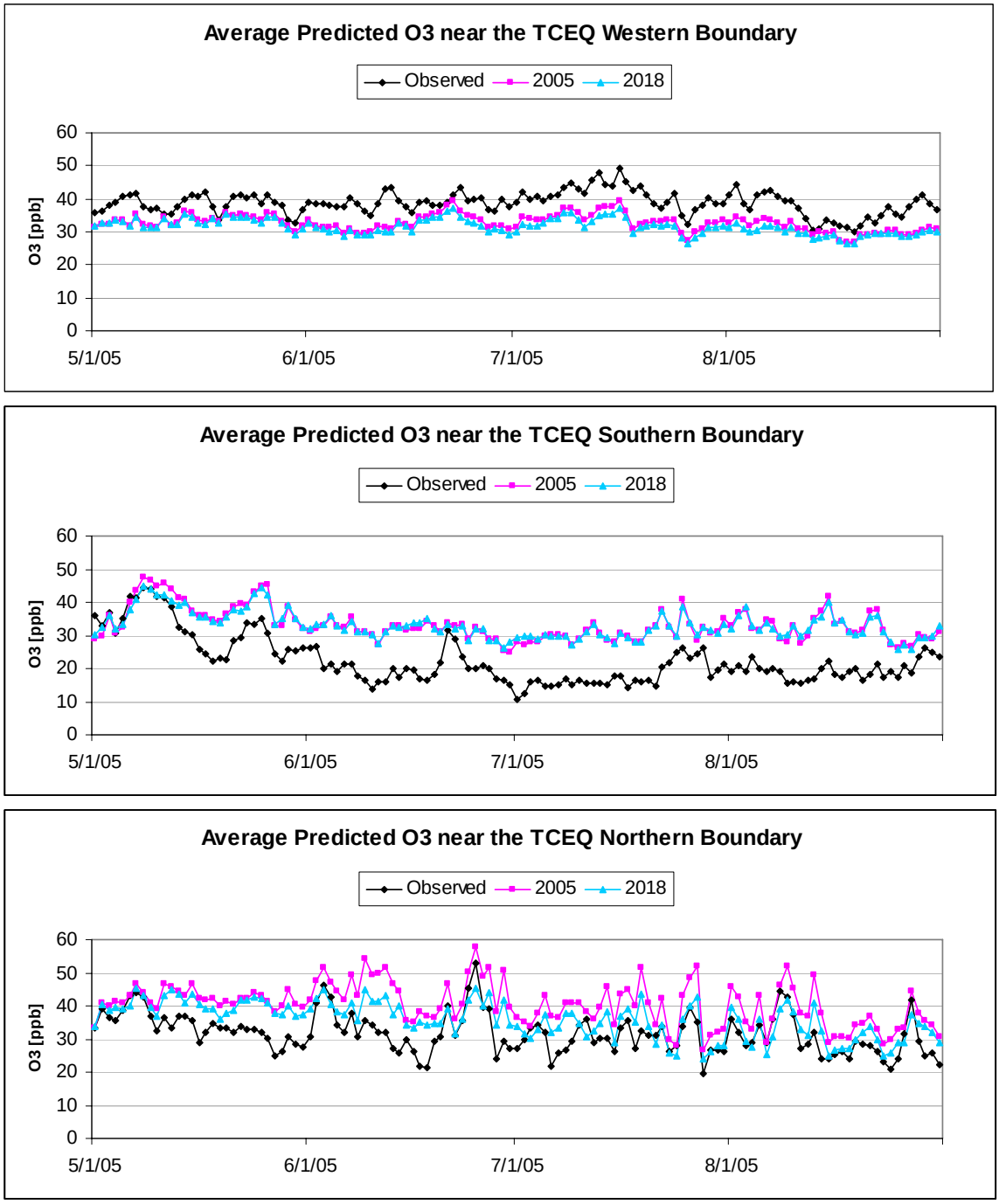

Figure 4-1. Time series of multi-site and daily averaged ozone in 2005 and 2018 near the western (top), southern (middle), and northern (bottom) boundaries of the TCEQ domain.

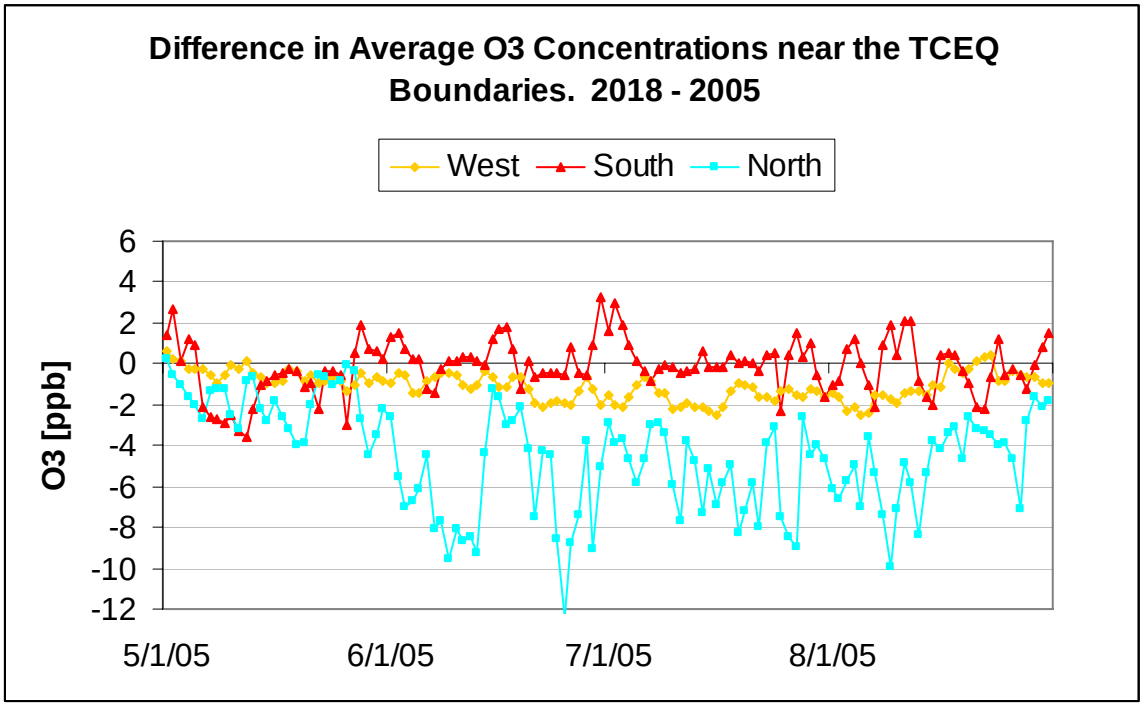

Figure 4-2. Time series of the differences in daily average O3 between 2005 and 2018 at sites near the TCEQ 36 km boundaries.

Figure 4-3 is similar to Figure 4-1, but shows time series of the daily average ozone from the 2006 base run using MOZART boundary conditions and its corresponding 2018 future year run. Differences between 2006 and 2018 near the three lateral boundaries are displayed in Figure 4-4.

The differences between 2006 and 2018 were comparable to the differences between 2005 and 2018. The future year western boundary was consistently 0 to 2 ppb lower than in the base year, averaging 1.4 and 1.1 ppb less in 2018 during the May 31 to June 16 and August to October episodes, respectively. Differences along the southern boundary fluctuated; the June episode increased 0.6 ppb while the August-October episode decreased 0.2 ppb. The northern boundary continued to show the greatest differences between the base and future years, averaging 3 ppb less ozone in the future year in both episodes.

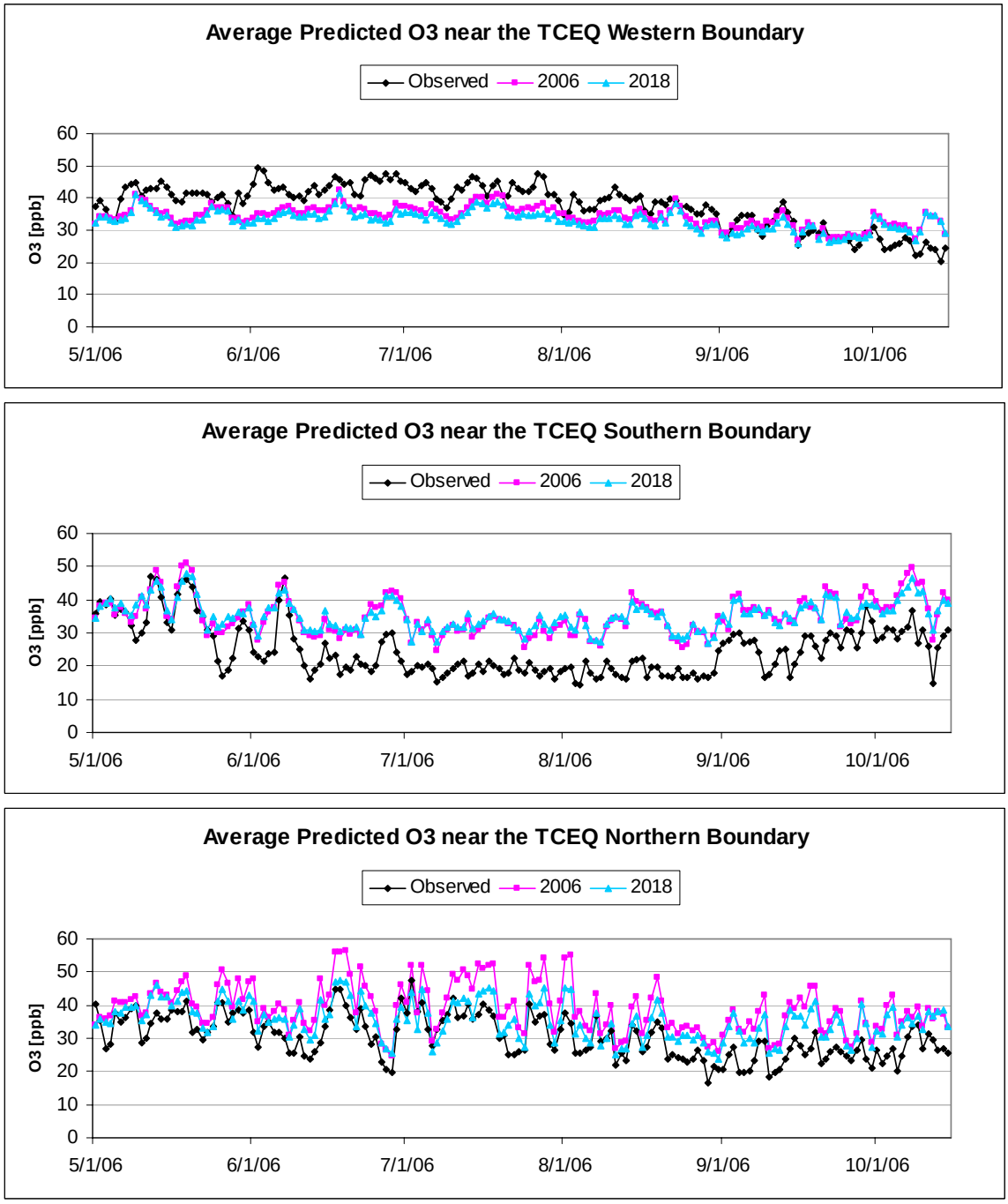

Figure 4-3. Time series of multi-site and daily averaged ozone in 2006 and 2018 near the western (top), southern (middle), and northern (bottom) boundaries of the TCEQ domain.

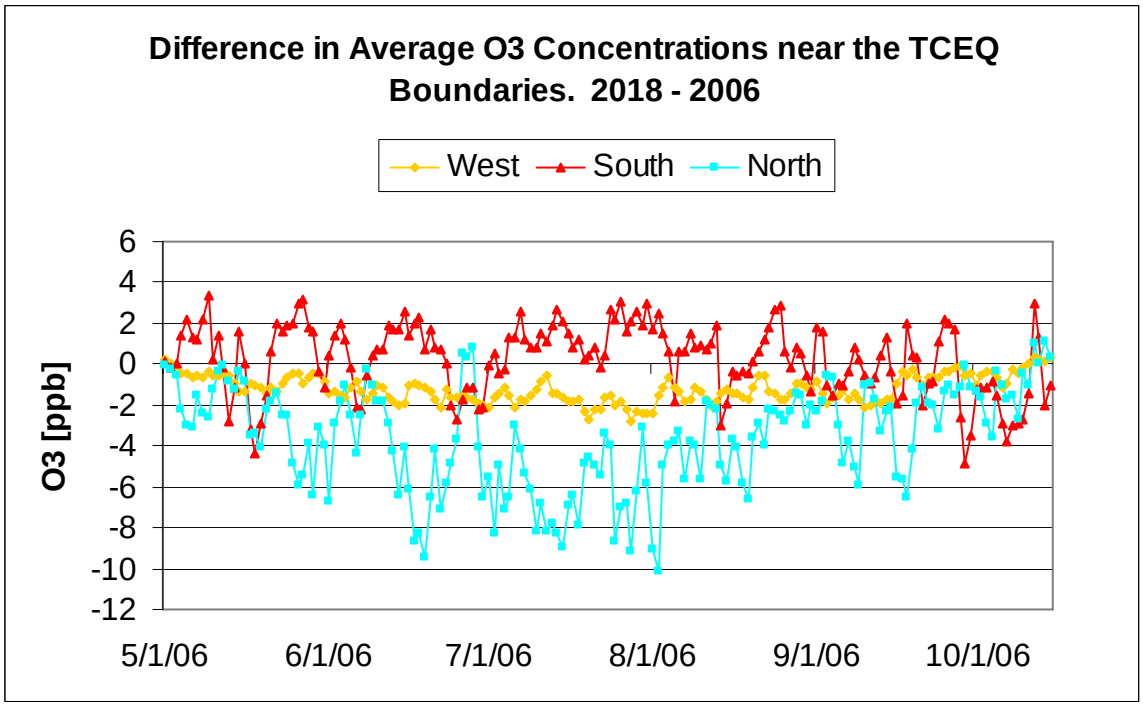

Figure 4-4. Time series of the differences in daily average O3 between 2006 and 2018 at sites near the TCEQ 36 km boundaries.

Differences in the base and future year runs were due to changes in the RPO inventory from 2005 or 2006 to 2018, and from the fire inventory. The former reduced NOx emissions by almost a third; the latter was based on different sources of fire emissions data. Additional modeling would be required to determine whether changes in the anthropogenic or fire inventories led to more changes in ozone near the TCEQ lateral boundaries.

Despite these changes, the daily average ozone near TCEQ's western boundary was very consistent between the base years and 2018, as surface ozone differed less than 2 ppb on almost all dates; most dates had less ozone in 2018. Results were mixed over the southern boundary most likely because there were very few monitoring sites used in the averaging. The northern boundary showed the largest reductions between the base and future year, including a 12 ppb difference in the June, 2005 episode. The high concentration of sites in Maine used to represent the northern boundary may explain the large difference.

REFERENCES

Bey, I., D. J. Jacob, R. M. Yantosca, J. A. Logan, B. D. Field, A. M. Fiore, Q. Li, H. Y. Liu, L. J. Mickley, and M. G. Schultz. 2001. Global modeling of tropospheric chemistry with assimilated meteorology: Model description and evaluation, *Journal of Geophysical Research* 106, 23,073–23,096.

Central States Air Resource Agencies and Central Regional Air Planning Association. 2004. "Research and Development of Planned Burning Emission Inventories for the Central States Regional Air Planning Association." Prepared by Sonoma Technology Inc. July.

Horowitz, L.W. et al. 2003. "A global simulation of tropospheric ozone and related tracers: Description and evaluation of MOZART, version 2." *Journal of Geophysical Research* 108, D24, 4784, doi:10.1029/2002JD002853.

Jaffe, D.; Chand, D.; Hafner, W.; Westerling, A.; and Spracklen, D. 2008. Influence of fires on O3 concentrations in the western US. *Environmental Science and Technology* 42, 5885-5891.

Karl, T. G.; Christian, T.J.; Yokelson, R.J.; Artaxo, P.; Hao, W.M.; and Guenther, A. 2007. The tropical forest and fire emissions experiment: method evaluation of volatile organic compound emissions measured by PTR-MS, FTIR, and GC from tropical biomass burning. *Atmos. Chem. Phys.*, 7, 8755-8793.

Western Governors Association/Western Regional Air Partnership. 2004. "2002 Fire Emission Inventory for the WRAP Region – Phase I – Essential Documentation." Prepared by Air Sciences Inc. Draft report. September.

Western Governors Association/Western Regional Air Partnership. 2005. "2002 Fire Emission Inventory for the WRAP Region – Phase II." Prepared by Air Sciences Inc. July.

Wiedinmyer, C.; Quayle, B.; Geron, C.; Belote, A.; McKenzie, D.; Zhang, X.; O'Neill, S.; Klos Wynne, K. 2006. Estimating emissions from fires in North America for air quality modeling. *Atmospheric Environment* 40, 3419-3432.

Zhang, X; Kondragunta, S.; Schmidt, C.; Kogan, F. 2008. Near real time monitoring of biomass burning particulate emissions (PM2.5) across contiguous United States using multiple satellite instruments. *Atmospheric Environment* 42, 6959-6972.